1959

A calculation of the elastic constants of yttrium and the rare earth metals

Benjamin Tobias Bernstein
Iowa State University

A CALCULATION OF THE ELASTIC CONSTANTS OF YTTRIUM AND THE RARE EARTH METALS

by

Benjamin Tobias Bernstein

A Dissertation Submitted to the
Graduate Faculty in Partial Fulfillment of
The Requirements for the Degree of
DOCTOR OF PHILOSOPHY

Major Subject: Physical Chemistry

Approved:

Signature was redacted for privacy.
In Charge of Major Work

Signature was redacted for privacy.
Head of Major Department

Signature was redacted for privacy.
Dean of Graduate College

Iowa State University
Of Science and Technology
Ames, Iowa

1959

TABLE OF CONTENTS

I. INTRODUCTION

The rare earth metals are a highly reactive, closely related group of elements (atomic numbers 57-71). Their close similarity, with the exceptions of cerium, europium, and ytterbium is accounted for by their basic electronic structures. All have the xenon atom core and three outer electrons in the 5d and 6s atomic levels. They differ only in the number of electrons in the 4f level. Although not actually members of the series, scandium and yttrium are generally included in any treatment of the rare earths because of their close chemical and physical similarities. Scandium and yttrium exhibit trivalent behavior with three valence electrons in the 3d and 4s, and 4d and 5s atomic levels, respectively. Experimental evidence (1) indicates that the 4f electrons are part of the atomic core for all the rare earth metals. Cerium has been postulated (2) to form quadrivalent atomic cores due to the promotion of the single 4f electron to the valence level. Experimental evidence (1) indicates that europium and ytterbium tend to half-fill and fill, respectively, the 4f level at the expense of the 5d and 6s atomic levels, forming divalent atomic cores.

The structure characteristics of the rare earth metals, scandium, and yttrium, compiled by Spedding et. al. (3), are given in Table 1. Scandium, yttrium, and most of the rare earth metals crystallize in the hexagonal close-packed

structure at room temperature. Lanthanum, praesodymium, and neodymium crystallize with a structure closely related to hexagonal close-packed. In this structure the basal planes are layered ABACABAC instead of the usual ABABABAB. Samarium crystallizes with a hexagonal structure which has a peculiar layering of close-packed planes. Cerium and ytterbium crystallize in the face-centered cubic structure. Europium crystallizes in the body-centered cubic structure. It is readily seen from Table 1 that cerium, europium, and ytterbium deviate from the other rare earth metals in the trend of decreasing mole atomic volume with increasing atomic number.

The polycrystalline elastic moduli of yttrium and eleven of the rare earth metals have been measured by Smith et. al. (4). The compressibility and shear modulus show an approximately linear trend with increasing atomic number for the hexagonal rare earth metals. The results for the compressibility and shear modulus of the metals investigated (4) are given in Table 2. Investigation of Table 2 reveals that cerium and ytterbium deviate drastically from the other rare earth metals. The compressibility is the reciprocal of the bulk modulus and is a measure of the interatomic forces resisting volume changes at zero shear. The shear modulus is a measure of the interatomic forces resisting deformation of shape at constant volume. The compressibility and shear modulus thus give complementary information about the interatomic forces in solids.

Table 1

Structure characteristics of the rare earth metals, scandium and yttrium

Element	Atomic number	Crystal structure	Lattice constants (Å) a	c	c/a	Mole at. vol. (cm^3)
La	57	hex	3.770	12.159	1.613[a]	22.544
Ce	58	f.c.c.	5.1612	--	--	20.705
Pr	59	hex	3.6725	11.8354	1.612[a]	20.818
Nd	60	hex	3.6579	11.7992	1.613[a]	20.590
Sm	62	hex	3.621	26.25	1.611[a]	19.950[a]
Eu	63	b.c.c.	4.606	--	--	29.423
Gd	64	h.c.p.	3.6360	5.7826	1.590	19.941
Tb	65	h.c.p.	3.6010	5.6936	1.581	19.258
Dy	66	h.c.p.	3.5903	5.6475	1.573	18.989
Ho	67	h.c.p.	3.5773	5.6158	1.570	18.745
Er	68	h.c.p.	3.5588	5.5874	1.570	18.458
Tm	69	h.c.p.	3.5375	5.5546	1.570	18.131
Yb	70	f.c.c.	5.4862	--	--	24.867
Lu	71	h.c.p.	3.5031	5.5509	1.585	17.768
Sc	21	h.c.p.	3.3090	5.2733	1.594	15.061
Y	39	h.c.p.	3.6474	5.7306	1.571	19.886

[a]Calculations based on h.c.p. unit cell.

Table 2

Compressibility and shear modulus of eleven of the rare earth metals

Element	Atomic number	Compressibility ($\times 10^6$ sq cm per kg)	Shear modulus ($\times 10^{-11}$ dynes per sq cm)
La	57	3.24	1.49
Ce	58	4.95	1.20
Pr	59	3.28	1.35
Nd	60	3.02	1.45
Sm	62	2.56	1.26
Gd	64	2.52	2.23
Tb	65	2.45	2.28
Dy	66	2.39	2.54
Ho	67	2.14	2.67
Er	68	2.11	2.96
Yb	70	7.12	0.70

The purpose of this investigation was to examine the observed variation with atomic number of the atomic radius and compressibility of the hexagonal rare earth metals and the deviation of cerium, europium and ytterbium from the above trends. Recently Smith and Gjevre (5) have measured the single crystal elastic constants of hexagonal close-packed yttrium in the temperature range 4.2°K to 400°K. A second

purpose of this investigation was to interpret the results for yttrium on the basis of a quantum mechanical theory of elasticity proposed by Fuchs (6) for the monovalent metals and developed by Leigh (7) and Reitz and Smith (8) for polyvalent metals. In addition an attempt was made to explain the observed variation with atomic number of the shear moduli of the hexagonal rare earth metals.

The application of the above theories of elasticity depends upon the assumption of nearly-free electron behavior of the valence electrons. A completely rigorous treatment of cohesion in the rare earths and related elements is not yet possible. In order to test the assumption of nearly-free electron behavior for the valence electrons of scandium, yttrium and the rare earth metals the cellular method as modified by Raimes (9) was extended to these elements. Raimes' method depends upon the assumption of equivalent valence electrons with nearly-free electron behavior. The term equivalent is taken to mean that the valence electrons share the same ground state wave functions and differ only in their wave-number vector, $\hat{k}$.

II. ANALYSIS OF ELASTIC STRESSES AND STRAINS

A. The Stress Tensor

A body which is acted on by external forces is said to be in a state of stress. If one considers a volume element situated within a stressed body, one may recognize two kinds of forces acting upon it. First, there are body forces, such as gravity, which act throughout the body and whose magnitudes are proportional to the volume of the element. Second, there are forces exerted on the surface of the element by the material surrounding it. These forces are proportional to the area of the surface of the element, and the force per unit area is called the stress. Stress may be represented by a second-rank tensor. The components T_{ij} of the stress tensor are defined as

$$T_{ij} = \lim_{\Delta A_j \to 0} \frac{\Delta F_i}{\Delta A_j} \quad (i,j = 1,2,3), \tag{1}$$

where the ΔF_i are components of the force acting on the surface element ΔA_j. A stress is said to be homogeneous if the forces acting on the surface of an element of fixed shape and orientation are independent of the position of the element in the body. The discussion in this work will be limited to states in which (a) the stress is homogeneous throughout the body, (b) all parts of the body are in statical

equilibrium, and (c) there are no body-torques.

The stress tensor is defined as:

$$(T_{ij}) = \begin{vmatrix} T_{11} & T_{12} & T_{13} \\ T_{21} & T_{22} & T_{23} \\ T_{31} & T_{32} & T_{33} \end{vmatrix} . \qquad (2)$$

The first subscript denotes the direction of the force and the second the normal to the plane to which the force is applied. T_{11}, T_{22}, and T_{33} are the normal components of the stress tensor and are tensions when positive. The non-diagonal components are the shear stresses. The condition that the body be in statical equilibrium and body-torques are absent imposes the condition for equilibrium that

$$T_{ij} = T_{ji} . \qquad (3)$$

The total number of independent stress components in equation 2 is reduced from nine to six by equation 3. The symmetrical stress tensor formed is given by:

$$(T_{ij}) = \begin{vmatrix} T_{11} & T_{12} & T_{13} \\ T_{12} & T_{22} & T_{23} \\ T_{13} & T_{23} & T_{33} \end{vmatrix} . \qquad (4)$$

B. The Strain Tensor

The variation of the displacement u_i with position x_i in a body, is used to define nine tensor components

$$\epsilon_{ij} = \frac{\partial u_i}{\partial x_j} \qquad (i,j = 1,2,3). \tag{5}$$

The ϵ_{ij} make up a second-rank tensor

$$(\epsilon_{ij}) = \begin{vmatrix} \epsilon_{11} & \epsilon_{12} & \epsilon_{13} \\ \epsilon_{21} & \epsilon_{22} & \epsilon_{23} \\ \epsilon_{31} & \epsilon_{32} & \epsilon_{33} \end{vmatrix}, \tag{6}$$

which may be separated into symmetrical and antisymmetrical parts by the relation,

$$(\epsilon_{ij}) = (e_{ij}) + (\omega_{ij}). \tag{7}$$

The strain tensor (e_{ij}) is defined as the symmetrical part of (ϵ_{ij}). The antisymmetrical part of (ϵ_{ij}), represented by (ω_{ij}), is known as the rotation. The components of (e_{ij}) and (ω_{ij}) are defined respectively by the relations

$$e_{ij} = \tfrac{1}{2}(\epsilon_{ij} + \epsilon_{ji})$$

and

$$\omega_{ij} = \tfrac{1}{2}(\epsilon_{ij} - \epsilon_{ji}). \tag{8}$$

If the strain is homogeneous and rotations are excluded, the strain tensor is defined as

$$(e_{ij}) = \begin{vmatrix} e_{11} & e_{12} & e_{13} \\ e_{12} & e_{22} & e_{23} \\ e_{13} & e_{23} & e_{33} \end{vmatrix}$$

$$= \begin{vmatrix} \epsilon_{11} & \frac{1}{2}(\epsilon_{12} + \epsilon_{21}) & \frac{1}{2}(\epsilon_{13} + \epsilon_{31}) \\ \frac{1}{2}(\epsilon_{12} + \epsilon_{21}) & \epsilon_{22} & \frac{1}{2}(\epsilon_{23} + \epsilon_{32}) \\ \frac{1}{2}(\epsilon_{13} + \epsilon_{31}) & \frac{1}{2}(\epsilon_{23} + \epsilon_{32}) & \epsilon_{33} \end{vmatrix}. \tag{9}$$

The e_{ii} are the normal (tensile) strains and are positive when the medium is extended. The e_{ij} are the shear components. One may interpret the shear components,

$$e_{ij} = \tfrac{1}{2}(\epsilon_{ij} + \epsilon_{ji}),$$

as composed of two simple strains. In one of the strains, planes of the material normal to the x_i axis slide in the x_j direction; in the other, planes normal to the x_j axis slide in the x_i direction. It should be noted that while the strain tensor is symmetrical and $e_{ij} = e_{ji}$ it is not necessarily true that $\epsilon_{ij} = \epsilon_{ji}$.

C. The Definition and Meaning of the Elastic Constants

If a general homogeneous stress T_{ij} is applied to a crystal the resulting homogeneous strain e_{ij} is such that each component is linearly related to all the components of the

stress for small displacements. This is a statement of Hooke's Law which may be written in the generalized tensor notation as,

$$e_{ij} = S_{ijkl}T_{kl}. \tag{10}$$

The constants of proportionality (S_{ijkl}) are called the elastic compliance constants. Alternatively, equation 10 may be written in the form:

$$T_{ij} = C_{ijkl}e_{kl}. \tag{11}$$

The constants of proportionality (C_{ijkl}) are now called the elastic constants, stiffness constants, or moduli of elasticity. It may be shown (10) that the exclusion of rotations and body-torques from consideration lead to constraints between the 81 components of the elastic constants such that

$$C_{ijkl} = C_{ijlk},$$

and

$$C_{ijkl} = C_{jikl}. \tag{12}$$

These constraints reduce the total number of independent constants from 81 to 36. The C_{ijkl} form a fourth-rank tensor.

It is customary to convert the tensor notation, used in the previous sections, to matrix notation. This is done in order to reduce the number of subscripts to enable ease of

handling in a particular problem. Both the stress components and the strain components are written as before, but with single subscripts running from 1 to 6:

$$\begin{vmatrix} T_{11} & T_{12} & T_{13} \\ T_{12} & T_{22} & T_{23} \\ T_{13} & T_{23} & T_{33} \end{vmatrix} \longrightarrow \begin{vmatrix} T_1 & T_6 & T_5 \\ T_6 & T_2 & T_4 \\ T_5 & T_4 & T_3 \end{vmatrix},$$

$$\begin{vmatrix} e_{11} & e_{12} & e_{13} \\ e_{12} & e_{22} & e_{23} \\ e_{13} & e_{23} & e_{33} \end{vmatrix} \longrightarrow \begin{vmatrix} e_1 & \frac{1}{2}e_6 & \frac{1}{2}e_5 \\ \frac{1}{2}e_6 & e_2 & \frac{1}{2}e_4 \\ \frac{1}{2}e_5 & \frac{1}{2}e_4 & e_3 \end{vmatrix}. \qquad (13)$$

The 36 elastic constants may be represented by the matrix:

$$(c_{ij}) = \begin{vmatrix} c_{11} & c_{12} & c_{13} & c_{14} & c_{15} & c_{16} \\ c_{21} & c_{22} & c_{23} & c_{24} & c_{25} & c_{26} \\ c_{31} & c_{32} & c_{33} & c_{34} & c_{35} & c_{36} \\ c_{41} & c_{42} & c_{43} & c_{44} & c_{45} & c_{46} \\ c_{51} & c_{52} & c_{53} & c_{54} & c_{55} & c_{56} \\ c_{61} & c_{62} & c_{63} & c_{64} & c_{65} & c_{66} \end{vmatrix}. \qquad (14)$$

The First Law of Thermodynamics for a volume under stress may be written in the form

$$dU = dQ + dW, \qquad (15)$$

where dU, dQ, and dW are respectively the change in internal energy, the heat change accompanying a displacement, and the

work done on the system during the displacement. If the deformation process is adiabatic, then $dQ = 0$ and the work done by the stress components T_i causing a strain de_i is

$$dW = T_i de_i. \tag{16}$$

The increase in internal energy may now be written in the form:

$$dU = dW = T_i de_i. \tag{17}$$

If Hooke's Law is obeyed then

$$dW = c_{ij} e_j de_i, \tag{18}$$

from which one obtains the relation:

$$(\partial W / \partial e_i) = c_{ij} e_j. \tag{19}$$

Equation 19 may be also derived if the deformation process is isothermal and reversible (10). Differentiating equation 19 with respect to e_j yields:

$$\partial / \partial e_j \, (\partial W / \partial e_i) = c_{ij}. \tag{20}$$

Since U is a function only of the state of the system, specified by the strain components, dW is a perfect differential for an adiabatic process. The order of differentiation in equation 20 is thus immaterial and

$$c_{ij} = c_{ji}. \tag{21}$$

The symmetry of the c_{ij} shown by equation 21 reduces the number of independent elastic constants from 36 to 21. Integrating equation 18 and using equation 21 the work necessary to produce a strain e_i, called the elastic strain energy W, is found to be:

$$W = W_o + \tfrac{1}{2}c_{ij}e_ie_j \tag{22}$$

per unit volume of the crystal. The number of independent elastic constants may be further reduced by the symmetry operations of the respective crystal classes (10,11). For hexagonal crystals, with which this work will be concerned, there are only five independent elastic constants represented by the matrix:

$$(c_{ij}) = \begin{vmatrix} c_{11} & c_{12} & c_{13} & 0 & 0 & 0 \\ c_{12} & c_{11} & c_{13} & 0 & 0 & 0 \\ c_{13} & c_{13} & c_{33} & 0 & 0 & 0 \\ 0 & 0 & 0 & c_{44} & 0 & 0 \\ 0 & 0 & 0 & 0 & c_{44} & 0 \\ 0 & 0 & 0 & 0 & 0 & \tfrac{1}{2}(c_{11}-c_{12}) \end{vmatrix}. \tag{24}$$

The most fundamental significance of the elastic constants, from an atomistic viewpoint, is their appearance as the second derivatives of the elastic strain energy. The

elastic strain energy of equation 22 is part of the complete thermodynamic potential of a crystal and hence directly related to the nature of the bonding in the crystal. Analysis of the elastic constants of metals in the light of current theory provides information concerning the interatomic forces in metals.

III. A MODIFIED CELLULAR CALCULATION FOR SCANDIUM, YTTRIUM AND THE RARE EARTH METALS

A. General Considerations

Wigner and Seitz (12) originated the cellular method for the calculation of the cohesive energies of metals. In this method a metal lattice is partitioned into a set of space-filling polyhedra which are centered about each of the metallic nuclei. The geometrical shape of these polyhedra, called cellular polyhedra, is dependent upon the symmetry of the crystal class to which the metal belongs. It is assumed that all electrons within a given cellular polyhedron may be divided into (a) inner electrons which are assumed to be rigidly attached to the nucleus and are not appreciably affected by changes in interatomic distances, and (b) outer electrons, chiefly responsible for the cohesion of the metal, which are affected by changes in interatomic distances. The inner electrons and the nucleus constitute an ion-core. The outer electrons are known as valence or conduction electrons. Each of the cellular polyhedra are electrically neutral. For simplicity of calculation Wigner and Seitz (12) have suggested that each cellular polyhedron be approximated by an atomic sphere of equal volume.

For a system containing N electrons, the many electron wave function may be described as

$$\Psi(\hat{x}_1,\hat{x}_2,\ldots,\hat{x}_N),$$

where $\hat{x}_1$, $\hat{x}_2$,..., $\hat{x}_N$ symbolize position vectors for the N electrons which also include the spin variables. The first and second order density matrices are defined by Brooks (13), using a notation due to Lowdin (14), as:

$$\Gamma(\hat{x}_1) = N\int|\Psi|^2 d\hat{x}_2\ldots.d\hat{x}_N, \tag{25}$$

$$\Gamma(\hat{x}_1,\hat{x}_2) = \frac{N(N-1)}{2}\int|\Psi|^2 d\hat{x}_3\ldots.d\hat{x}_N, \tag{26}$$

where the integrations are taken over all the electronic coordinates except those which occur explicitly in the argument of the Γ's and summation over spin variables is understood. The joint density matrix is defined as:

$$\Gamma(\hat{x}_1'|\hat{x}_1) = N\int\Psi^*(\hat{x}_1',\hat{x}_2,..\hat{x}_N)\Psi(\hat{x}_1,\hat{x}_2,\ldots,\hat{x}_N)d\hat{x}_2\ldots d\hat{x}_N, \tag{27}$$

in which the wave functions in the integrand differ in the position of electron 1.

If the wave function Ψ is written as an antisymmetrized sum of products given by

$$\Psi(x_1,x_2,\ldots,x_N) = \sum_{k=1}^{N}\phi_{k1}(\hat{x}_1)\phi_{k2}(\hat{x}_2)\ldots.\phi_{kN}(\hat{x}_N), \tag{28}$$

then equation 27 becomes

$$\Gamma(\hat{x}_1' | \hat{x}_1) = \sum_{k=1}^{N} \int \phi_k^*(\hat{x}_1') \phi_k(\hat{x}_1) d\hat{x}_2 \ldots d\hat{x}_N, \tag{29}$$

and equation 25 becomes

$$\Gamma(\hat{x}_1) = \sum_{k=1}^{N} \int |\phi_k(\hat{x}_1)|^2 d\hat{x}_2 \ldots d\hat{x}_N. \tag{30}$$

The second order density matrix, equation 26, now has the form

$$\Gamma(\hat{x}_1, \hat{x}_2) = \tfrac{1}{2}\Gamma(\hat{x}_1)\Gamma(\hat{x}_2) - \tfrac{1}{2}|\Gamma(\hat{x}_1 | \hat{x}_2)|^2. \tag{31}$$

The total energy of a metal at the absolute zero of temperature may be written in the cellular approximation as

$$\begin{aligned} E = & -\sum_{k=1}^{N} \int \phi_k(\hat{x}_1) \nabla^2 \phi_k(\hat{x}_1) d\tau_1 \\ & + \sum_{k=1}^{N} \int \phi_k(\hat{x}_1) V(\hat{x}_1) \phi_k(\hat{x}_1) d\tau_1 \\ & + 2 \int \frac{\Gamma(\hat{x}_1, \hat{x}_2) - \tfrac{1}{2}\Gamma(\hat{x}_1)\Gamma(\hat{x}_2)}{r_{12}} d\tau_1 d\tau_2 \\ & + \tfrac{1}{2} \sum_{g,h} V_{gh} + \sum_{g,k} \epsilon_{gk}. \end{aligned} \tag{32}$$

The first term in equation 32 is the kinetic energy of the valence electrons. The second term is the sum of (a) the potential energy due to the interaction of an ion-core with

the negative charge inside an atomic polyhedron, and (b) the self-potential energy of the valence electron charge distribution within an atomic polyhedron. The third term involves the joint probability density of equation 29 and gives rise to what are known as the exchange and correlation energies. The integrations are taken over the volume of the atomic sphere representing the cellular polyhedron. The quantity r_{12} denotes the distance between electrons 1 and 2. The fourth term in equation 32 is the non-Coulomb interaction energy of the rigid ion-cores due to the overlapping of the core shell electrons between cells g and h. The fifth and final term is the electrostatic potential energy due to the non-spherically symmetrical part of the electronic charge distribution and corresponds to the sum of (a) the interaction of the non-spherically symmetric part of the charge distribution in cell h with the potential produced by the net ion-core charge in cell g, and (b) the interaction of the total charge distribution in cell g with the potential produced by the non-spherically symmetric part of the charge distribution in cell h. The reader is referred to the articles by Brooks (13) and Reitz (15) for detailed treatments of how the various terms in equation 32 enter into the expression for the total energy of a metal. A comprehensive discussion of the exchange and correlation energies is given in an article by Pines (16). The zero point energy, core polarization effects, and multipole inter-

actions are neglected in equation 32. The one-electron wave functions may be represented in the form developed by Bloch (17) as

$$\phi_j = \phi_k \exp i\hat{k} \cdot \hat{r}, \tag{33}$$

where $\hat{r}$ is a position vector, $\hat{k}$ is a wave-number vector and ϕ_k has the translational periodicity of the lattice.

The Bohr system of units was used throughout the course of this investigation unless otherwise indicated. For this system the unit of energy is the rydberg (1Ry = 13.60 eV), and the unit of length is the radius (0.5292×10^{-8} cm) of the first Bohr orbit in a hydrogen atom of infinite nuclear mass.

B. The Modified Cellular Method of Raimes

The Schrodinger wave equation for an electron in a metal, neglecting the last three terms in equation 32, may be written as

$$\nabla^2\phi_j + \left(\epsilon_j - V(r)\right)\phi_j = 0 \tag{34}$$

where ϕ_j is a Bloch wave of equation 33. Calculations of ϕ_k in magnesium (18) indicate that in divalent as well as monovalent metals ϕ_k is very flat near to the boundary of the atomic sphere representing the cellular polyhedron and approximately constant over much of the volume. Thus equation

33 may be written as

$$\phi_j = \phi_o \exp i\hat{k} \cdot \hat{r}, \tag{35}$$

with the assumption that ϕ_k is equal to a constant value ϕ_o. The function ϕ_o is the wave function for the state of lowest energy. Equation 34 may now be written in terms of ϕ_o as

$$\nabla^2\phi_o + 2i\hat{k}j \cdot (\nabla\phi_o) + (\epsilon_j - k_j^2 - V)\phi_o = 0. \tag{36}$$

Since ϕ_o is assumed constant, $\nabla\phi_o$ vanishes and ϵ_j is given by

$$\epsilon_j = E_o + \frac{h^2}{2m} k^2. \tag{37}$$

E_o corresponds to the sum of the first two terms in equation 32 and consists of the kinetic energy of the electrons in the lowest state, the potential energy due to the interaction of an electron with the ion-core field in an atomic polyhedron, and the self-potential energy of the valence electron charge distribution within an atomic polyhedron. The mean value of $[(h^2/2m)\ k^2]$ is called the mean Fermi energy, since it corresponds to the mean additional kinetic energy that the valence electrons would possess in the solid as compared to the free atom and is due to a Fermi-Dirac distribution.

Calculation of ϕ_o by Raimes (18) for magnesium, using a self-consistent field of the Hartree type for the Mg^{+2} ion, showed that ϕ_o did not give significantly different results for

the total energy if the self-potential of the conduction electrons was due to electrons with one type of spin only or to electrons with two different types of spin. This result suggested (9) that the neglect of spin variables leads to only a slight reduction in accuracy in calculating the total energy of a polyvalent metal. On this basis, E_o may be calculated using the ion-core potential, as for the monovalent metals, plus the self-potential energy of the valence electron charge distribution within an atomic sphere due to electrons with one type of spin only. On this basis one may write E_o of equation 37 as

$$E_o = \epsilon_o + \epsilon_c, \tag{38}$$

where ϵ_o is the sum of the kinetic and ion-core potential energies of the lowest state and ϵ_c is the self-potential energy of the valence electron charge distribution within the volume of the sphere corresponding to the unit polyhedron. It should be emphasized that ϵ_c is calculated on the basis of electrons with one type of spin only.

The boundary condition for the determination of ϵ_o may be written in the form

$$\left(\frac{d\phi_o}{dr}\right)_{r=r_s} = 0 \tag{39}$$

where ϕ_o is the solution of the radial Schrodinger wave equation,

$$\frac{d^2\phi_o}{dr^2} + \frac{2}{r}\frac{d\phi_o}{dr} + \left[\epsilon_o(r_s) - V(r)\right]\phi_o = 0, \qquad (40)$$

for the state of lowest energy, and r_s is the radius of the atomic sphere. In order to evaluate $\epsilon_o(r_s)$ for atomic radii in the neighborhood of r_o, where r_o is the value of r_s for which ϵ_o reaches its minimum, it must be assumed that in the range of r_s of interest the ion-core potential is Coulombic and that $V(r) = -2\nu/r$, where ν is the valence of the multiply charged ion. Writing $R = r\phi_o$, equation 40 becomes

$$\frac{d^2R}{dr^2} + \left[\epsilon_o(r_s) - V(r)\right]R = 0 \qquad (41)$$

and the boundary condition, equation 39, becomes

$$\left(\frac{dR}{dr}\right)_{r=r_s} = \frac{R}{r} . \qquad (42)$$

Through equation 42 it is seen that R is a function of r_s as well as of r. The assumption was made (9) that ϕ_o is nearly constant. The charge density at the surface of an atomic sphere was assumed equal to the mean charge density taken over the volume of the sphere by fulfilling the condition:

$$\frac{4\pi r_s^3}{3}\left|\phi_o(r_s)\right|^2 = \frac{4\pi r_s}{3}\left|R(r_s)\right|^2 = 1. \qquad (43)$$

Raimes (9) has shown that by reason of equations 41, 42, and 43 one obtains

$$\frac{d\epsilon_o}{dr_s} = \frac{3}{r_s}\left[V(r_s) - \epsilon_o\right], \tag{44}$$

which may be integrated to obtain

$$\epsilon_o(r_s) = \nu\left(\frac{r_o^2}{r_s^3} - \frac{3}{r_s}\right), \tag{45}$$

provided that $V(r_s) = -2\nu/r_s$. The repulsive interaction of the ion-core shells, V_{gh} of equation 32, and the non-spherical part of the electrostatic charge distribution, ϵ_{gk} of equation 32, give negligible contributions to the total energy of a metal in which the clearance between ion-cores is large (19). By regrouping terms in equation 32 the total energy of a metal, per valence electron, may be expressed (13) in terms of the valence of the ion-core as

$$E(r_s) = \nu\left(\frac{r_o^2}{r_s^3} - \frac{3}{r_s}\right) + \frac{1.2\nu}{r_s} + \frac{2.21\nu^{2/3}}{r_s^2} - \frac{0.916\nu^{1/3}}{r_s} - \nu^{\frac{1}{2}} g\left(\frac{r_s}{\nu^{-2/3}}\right), \tag{46}$$

the terms having been kept separate for identification. The first term in equation 46 is the energy of the lowest state, ϵ_o of equation 45. The second term is the self-potential energy of the valence electron charge distribution within an atomic sphere assuming a uniform charge distribution as for free electrons. The third and fourth terms are, in order, the Fermi and exchange energies calculated according to the free electron approximation as given by Seitz (19). The last

term in equation 46 is the correlation energy for free electrons, given by the Wigner relationship (13) as

$$g(r_s) = \frac{-0.916}{r_s} - 0.114 + 0.0313 \ln r_s + 0.0005 r_s. \qquad (47)$$

If r_o is known one may solve for r_s in equation 46, at the equilibrium value ρ, by the condition that

$$\left(\frac{dE}{dr_s}\right)_{r_s=\rho} = 0. \qquad (48)$$

Raimes (9) has shown that r_o may be calculated for divalent and trivalent metals by means of the second and third empirical ionization energies, respectively, of the free neutral atoms. For a divalent metal, r_o may be calculated from the relation (9)

$$r_o^2 - \frac{2+\omega}{\omega^3} r_o + \frac{(2-\omega)^2}{\omega^5} + \left[\frac{r_o}{\omega} - \frac{3(3-\omega)}{2\omega^4}\right] \xi \cot \xi = 0, \qquad (49)$$

where $\xi = (4r_o - \omega^2 r_o^2)^{\frac{1}{2}}$ and $\omega^2 = I_2$, the negative of the second empirical ionization potential for a free neutral atom. For a trivalent metal (20) r_o is given by

$$r_o^2 - \frac{3(3+\omega)}{2\omega^3} r_o + \frac{3(3-\omega)^2}{2\omega^5} + \left[\frac{r_o}{\omega} - \frac{3(3-\omega)}{2\omega^4}\right] \xi \cot \xi = 0, \qquad (50)$$

where $\xi = (6r_o - \omega^2 r_o^2)^{\frac{1}{2}}$ and $\omega^2 = I_3$, the negative of the

third empirical ionization potential of a free neutral atom. It should be emphasized that the treatment of all the valence electrons as free and equivalent is essential to the derivation and validity of equations 48, 49, and 50.

C. Procedure and Results for Scandium, Yttrium and the Rare Earth Metals

The predominantly trivalent chemical behavior observed in scandium, yttrium and most of the rare earth metals as contrasted to the large number of oxidation states observed in other transition metals, such as manganese, suggests that the approximation of considering all the valence electrons on an equivalent basis may be valid for these elements.

Additional support for the application of this approximation to the rare earths and related metals comes from the recent work of Altmann (21) and Altmann and Cohan (22) on the energy levels at the center of the Brillouin zone for zirconium and titanium, respectively. The cellular method was applied in the above investigations without introducing the sphere approximation for the cellular polyhedron. A computer program was developed (21) for the least squares fitting of the boundary conditions. The results for titanium and zirconium show that there are four d states lying very near the s ground state in the solid. The proximity of the first d level to the ground state agrees

with the assumption that all four valence electrons have metallic behavior. Altmann (21) and Altmann and Cohan (22) suggest that a considerable amount of s-d hybridization is occurring in zirconium and titanium due to the proximity of the s and d levels in the solid state.

In order to calculate the atomic radius, total energy, and compressibility of a metal from equation 46 the value of the constant r_o must be known. The constant r_o may be determined for divalent or trivalent metals by means of the appropriate empirical ionization potential for the free neutral atom and the use of equations 49 or 50, respectively. The values of the third empirical ionization potentials needed to solve equation 50 were not available for the trivalent rare earth metals with the exception of lanthanum. The third empirical ionization potentials for scandium and yttrium were available. A method was developed to calculate r_o for those elements for which the empirical ionization potentials were not known. This method was based upon the construction of a potential from the ion-core within an atomic sphere and the utilization of the empirical ionic radii of the trivalent rare earth ions. The usual assumptions of Raimes' method (9) were made; namely, that (a) the ion-core is that of the atom stripped of all its valence electrons, (b) the core electrons are unperturbed in going from the free neutral atom to the solid, and (c) the valence electrons are equivalent.

A potential due to the ion-core was constructed on the basis of the boundary conditions:

$$-rV(r) = 2Z + ar + br^2 \qquad r \leqslant r_o, \tag{51}$$

$$-rV(r) = 2\mathcal{N} \qquad r \gtrsim r_o. \tag{52}$$

The form of equations 51 and 52 is analogous to the potential functions used by Prokofjew (23) for sodium and Schiff (24) for titanium. In equations 51 and 52, r_o corresponds to the equilibrium cell radius for the state of lowest energy, Z is the atomic number, a and b are two adjustable parameters dependent upon the boundary conditions, and $\mathcal{N}$ is the valence of the multiply charged ion-core. Since the ion-core potential and its derivative must be continuous at the boundary of the atomic sphere, the boundary condition is imposed upon equation 51 that

$$\frac{d}{dr}\left[-rV(r)\right]_{r=r_o} = 0. \tag{53}$$

The values of a and b obtained from equations 51, 52, and 53 are:

$$a = -2br_o, \tag{54}$$

$$b = 2(Z-\mathcal{N})/r_o^2. \tag{55}$$

Substituting the above values of a and b into equation 51 leads to the relation

$$-rV(r) = 2Z - 4(Z - \mathcal{N})r/r_o + 2(Z - \mathcal{N})r^2/r_o^2. \tag{56}$$

It is readily seen that the potential in equation 56 is proportional to the atomic number close to the nucleus and is proportional to the net-core charge at the cell boundary. It is also interesting to note that through equation 56 the potential from the ion-core is a function of r_o as well as of r.

The magnitude of the potential from the ion-core within an atomic sphere decreases from the nucleus to the cell boundary. At the ionic radius it should be equal to the atomic number minus a screening number for the core shell electrons. On the basis of this approximation the effective potential from the ion-core at the ionic radius r_c is given by

$$\left[-rV(r)\right]_{r=r_c} = 2(Z-S), \tag{57}$$

where S is a screening number for the outermost core shell in the solid. The empirical ionic crystal radii of the trivalent rare earth ions (25) are given in Table 3. A relation between r_o, r_c, and S was obtained from equations 56 and 57. This relation is:

$$r_o^2 - 2(Z-\nu)\frac{r_c r_o}{S} + (Z-\nu)\frac{r_c^2}{S} = 0. \tag{58}$$

On the basis of equation 58 it is seen that the spherically symmetric ion-core potential within the atomic sphere representing the cellular polyhedron is dependent only upon

Table 3

Empirical ionic crystal radii for the trivalent rare earth ions

Ion	Ionic radius (Bohr units)
La^{+3}	2.00
Ce^{+3}	1.95
Pr^{+3}	1.91
Nd^{+3}	1.87
Pm^{+3}	1.83
Sm^{+3}	1.81
Eu^{+3}	1.80
Gd^{+3}	1.76
Tb^{+3}	1.74
Dy^{+3}	1.70
Ho^{+3}	1.68
Er^{+3}	1.66
Tm^{+3}	1.63
Yb^{+3}	1.61
Lu^{+3}	1.59

the atomic number, the ionic radius, the constant r_o, and the screening number of the outermost core shell. The approximation is now made that the difference between the cell

radius r_o and the ionic radius r_c is constant for all the trivalent rare earth metals. The empirical third ionization potential of 1.4158 Ry (26) for lanthanum was used to calculate r_o as 3.47 Bohr units by means of equation 50. Using this value of r_o for lanthanum and the empirical ionic radius of 2.00 Bohr units obtained from Table 3, the constant $(r_o - r_c)$ was found to be 1.47 Bohr units. This approximation results in the following relationship for r_o for the trivalent rare earth metals:

$$r_o = 1.47 + r_c, \tag{59}$$

where the values of r_c needed to solve equation 59 are given in Table 3.

In order to calculate r_o for europium and ytterbium in which the 4f shell is presumed half-filled and filled, respectively, the assumption is made that the ion-cores are divalent in the solid state. The screening number S for the divalent ion-core of the element of next highest atomic number, since in europium and ytterbium the divalent state is presumed to arise from the demotion of one valence electron to the 4f core shell. The ionic crystal radius for the divalent metal may be approximated (27) from the relation

$$r_{+2} = r_{+3} \frac{(Z - S)_{+3}}{(Z - S)_{+2}} \left(\frac{3}{2}\right)^{2/n-1} . \tag{60}$$

In equation 60, n is an exponent which is related to the repulsive forces arising from the interpenetration of the ions. The value of n for a xenon or pseudo-xenon core is given by Pauling (27) as 12. The screening numbers for the rare earth ions in the solid state were obtained from equations 58, 59, and the empirical ionic radii of Table 3. The screening numbers of the rare earth ions in the solid state are given in Table 4. A similar development was used for cerium with the quadrivalent ionic crystal radius being determined from the relation (27)

$$r_{+4} = r_{+3} \frac{(Z - S)_{+3}}{(Z - S)_{+4}} \left(\frac{3}{4}\right)^{2/n-1} . \qquad (61)$$

Ionic radii for divalent europium and ytterbium of 2.01 and 1.81 Bohr units, respectively, were obtained from equation 60 by substitution of the appropriate values from Tables 3 and 4. Once r_c and S have been determined for the divalent metal it is a simple matter to calculate r_o from equation 58. The calculated equilibrium atomic radii for the state of lowest energy of the rare earth metals plus scandium and yttrium are given in Table 5. The values of r_o for scandium and yttrium in Table 5 were evaluated from equation 50 through use of the third ionization potentials (26) of 1.820 and 1.514 Ry, respectively. The second ionization potential of europium was available from the compilation of Sherman (28). A value of r_o for europium was

Table 4

Calculated screening numbers for the rare earth ions in the solid state

Ion	Screening number
La^{+3}	44.31
Ce^{+3}	44.84
Ce^{+4}	44.31
Pr^{+3}	45.41
Nd^{+3}	45.96
Pm^{+3}	46.49
Sm^{+3}	47.15
Eu^{+3}	47.88
Eu^{+2}	48.37
Gd^{+3}	48.37
Tb^{+3}	49.00
Dy^{+3}	49.46
Ho^{+3}	50.06
Er^{+3}	50.57
Tm^{+3}	51.16
Yb^{+3}	51.74
Yb^{+2}	52.31
Lu^{+3}	52.31

Table 5

Calculated equilibrium atomic radii for the state of lowest energy of the rare earth metals, scandium, and yttrium

Element	Atomic number	r_o (Bohr units)
La	57	3.47
Ce[a]	58	3.42
Ce[b]	58	3.09
Pr	59	3.38
Nd	60	3.34
Pm	61	3.30
Sm	62	3.28
Eu[c]	63	3.67
Eu[d]	63	3.66
Gd	64	3.23
Tb	65	3.21
Dy	66	3.17
Ho	67	3.15
Er	68	3.13

[a]Trivalent; calculated from equation 59.

[b]Quadrivalent; calculated from equations 58 and 61.

[c]Divalent; calculated from equations 58 and 60.

[d]Divalent; calculated from equation 49.

Table 5. (Continued)

Element	Atomic number	r_o (Bohr units)
Tm	69	3.10
Yb[c]	70	3.38
Lu	71	3.06
Sc[e]	21	2.56
Y[e]	39	3.20

[e]Calculated from equation 50.

evaluated from equation 49 and the second empirical ionization potential of 0.838 Ry.

The equilibrium atomic radii were obtained from equations 46 and 48 using the values of r_o given in Table 5. The adiabatic compressibility, K, at 0°K is the reciprocal of the bulk modulus B and is obtained from equation 46 at the equilibrium radius by the relation

$$\frac{1}{K} = B = \left(\frac{\partial^2 E}{\partial V^2}\right)_{0°K} . \tag{62}$$

The total energy of a metal was calculated from equation 46 at the equilibrium atomic radius. The cohesive energy of a metal was calculated as the difference between the total energy of the solid and the ionization energy of an equivalent number of valence electrons in the free neutral atoms. The calculated

atomic radii, compressibilities, total energies, and cohesive energies of the rare earth metals, scandium, and yttrium at 0°K are given in Table 6. The available experimental data are also listed for comparison. The observed atomic radii at room temperature, with the exception of quadrivalent cerium, were obtained from the data of Spedding et. al. (3). The atomic radius of quadrivalent cerium was obtained from the work of Lawson and Tang (2). The observed adiabatic compressibilities at room temperature, with the exception of yttrium, were obtained from the data of Smith et. al. (4). The observed adiabatic compressibility of yttrium at 4.2°K was obtained from the single crystal elastic constants (5). The isothermal compressibilities given in Table 6, with the exception of europium and quadrivalent cerium, were obtained from the room temperature data of Bridgman (29). The isothermal compressibility of quadrivalent cerium was obtained from Swenson* and the corresponding value for europium from the compilation by Gschneidner (30). The observed cohesive energies at 298°K were obtained from the compilation of Wigner and Seitz (31) for lanthanum, cerium, scandium, and yttrium. The observed cohesive energies for the rest of the rare earth metals at 0°K were obtained from the results of Trulson (32).

---

*Swenson, C. A., Ames, Iowa. The compressibility of cerium. Private communication. 1959.

Table 6

Atomic radii, compressibilities, total energies, and cohesive energies for the rare earth metals, scandium, and yttrium

Element	Atomic number	Atomic radius (Å)		Compressibility ($\times 10^6$ cm^2/kg)			Total energy (kcal/mol)		Cohesive energy (kcal/mol)	
		Calc.	Obs.	Calc.	Obs.[a]	Obs.[b]	Calc.	Obs.	Calc.	Obs.
La	57	2.49	2.08	3.47	3.24	3.9	888	922	54	88
Ce[c]	58	2.46	2.02	3.29	4.95	4.7	892	--	--	84
Ce[d]	58	2.28	1.89	1.58	--	3.5	1636	--	--	--
Pr	59	2.44	2.02	3.21	3.28	3.7	905	--	--	85
Nd	60	2.42	2.01	3.14	3.02	3.0	912	--	--	77
Pm	61	2.40	--	3.06	--	--	921	--	--	--

[a]Adiabatic measurements.

[b]Isothermal measurements.

[c]Assumed trivalent.

[d]Assumed quadrivalent.

Table 6. (Continued)

Element	Atomic number	Atomic radius (Å)		Compressibility (x 10^6 cm^2/kg)			Total energy (kcal/mol)		Cohesive energy (kcal/mol)	
		Calc.	Obs.	Calc.	Obs.[a]	Obs.[b]	Calc.	Obs.	Calc.	Obs.
Sm	62	2.38	1.99	2.88	2.56	3.5	926	--	--	50
Eu	63	2.56	2.27	8.13	--	7.5	415	435	23	43
Gd	64	2.35	1.99	2.78	2.52	2.5	935	--	--	82
Tb	65	2.34	1.97	2.74	2.45	--	939	--	--	--
Dy	66	2.32	1.96	2.65	2.39	2.6	948	--	--	72
Ho	67	2.30	1.95	2.57	2.14	2.5	952	--	--	75
Er	68	2.29	1.94	2.52	2.11	2.5	957	--	--	76
Tm	69	2.27	1.93	2.47	--	2.6	963	--	--	58
Yb	70	2.40	2.14	6.33	7.12	7.5	438	--	--	40
Lu	71	2.25	1.92	2.36	--	2.3	972	--	--	94
Sc	21	1.95	1.81	1.37	--	--	1102	1104	91	93
Y	39	2.33	1.99	2.69	2.31	--	944	1000	47	103

The experimental and calculated atomic radii are plotted against atomic number for the hexagonal rare earth metals in Figure 1. A similar plot of the calculated adiabatic compressibility versus atomic number is shown in Figure 2, in comparison to the results obtained by Smith et. al. (4).

Screening number of 28.51 and 15.08 for the trivalent ions of yttrium and scandium, respectively, were evaluated from equation 58 by substitution of the appropriate values of r_o from Table 5 and the empirical ionic radii (33) of 1.74 and 1.53 Bohr units. The calculated screening numbers for the trivalent ions of lanthanum and yttrium of 44.31 and 28.51, respectively, compare favorably with the values of 43.30 and 27.35 estimated for the free ions (34). An estimated screening number of 11.11 for the free trivalent scandium ion (34) is in poor agreement with the calculated value of 15.08 for the solid.

Figure 1. Variation of atomic radius with atomic number for the hexagonal rare earth metals

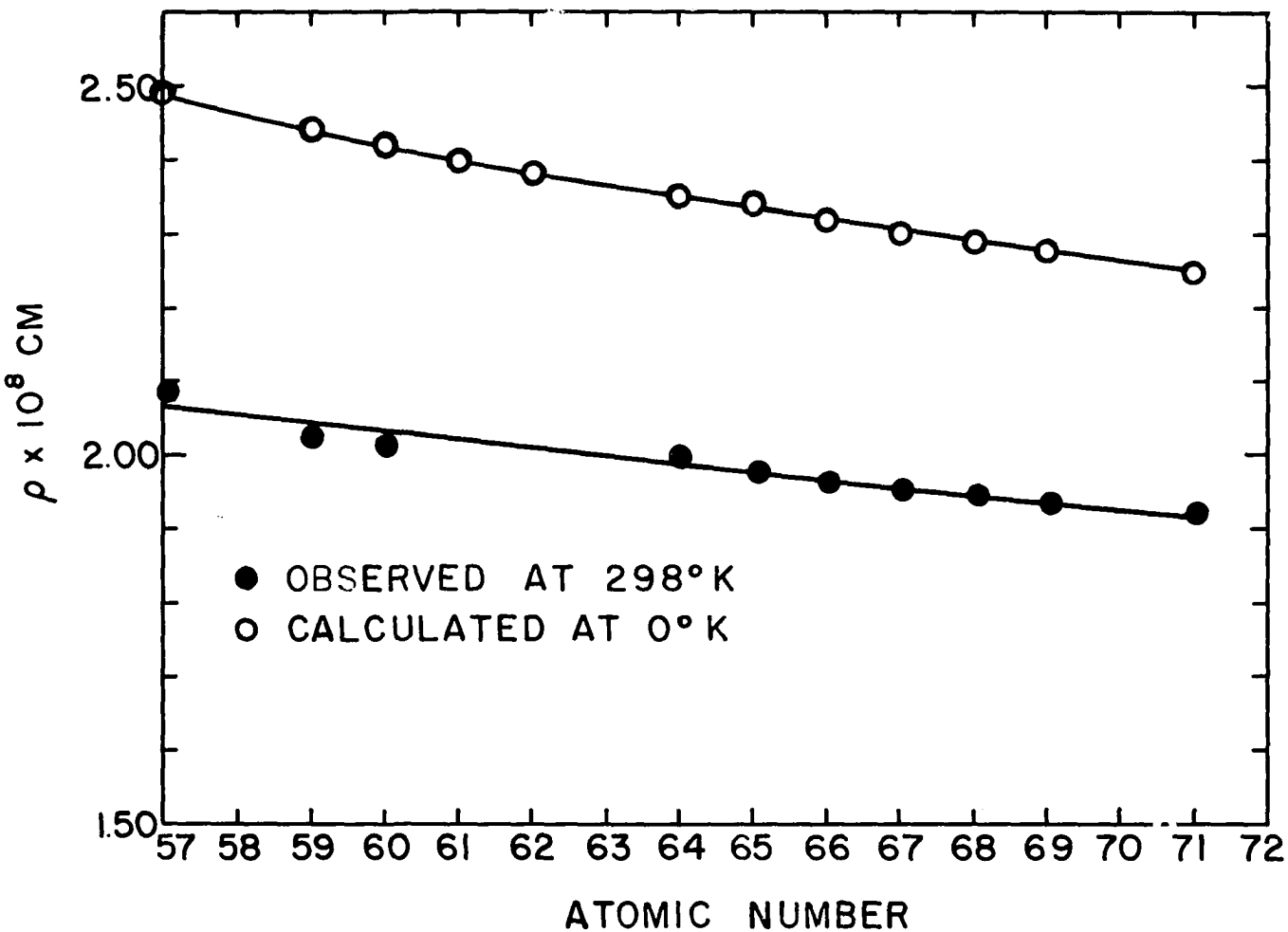
2.50
2.00
1.50
ρ x 10⁸ CM
● OBSERVED AT 298°K
○ CALCULATED AT 0°K
57 58 59 60 61 62 63 64 65 66 67 68 69 70 71 72
ATOMIC NUMBER

Figure 2. Variation of adiabatic compressibility with atomic number for the hexagonal rare earth metals

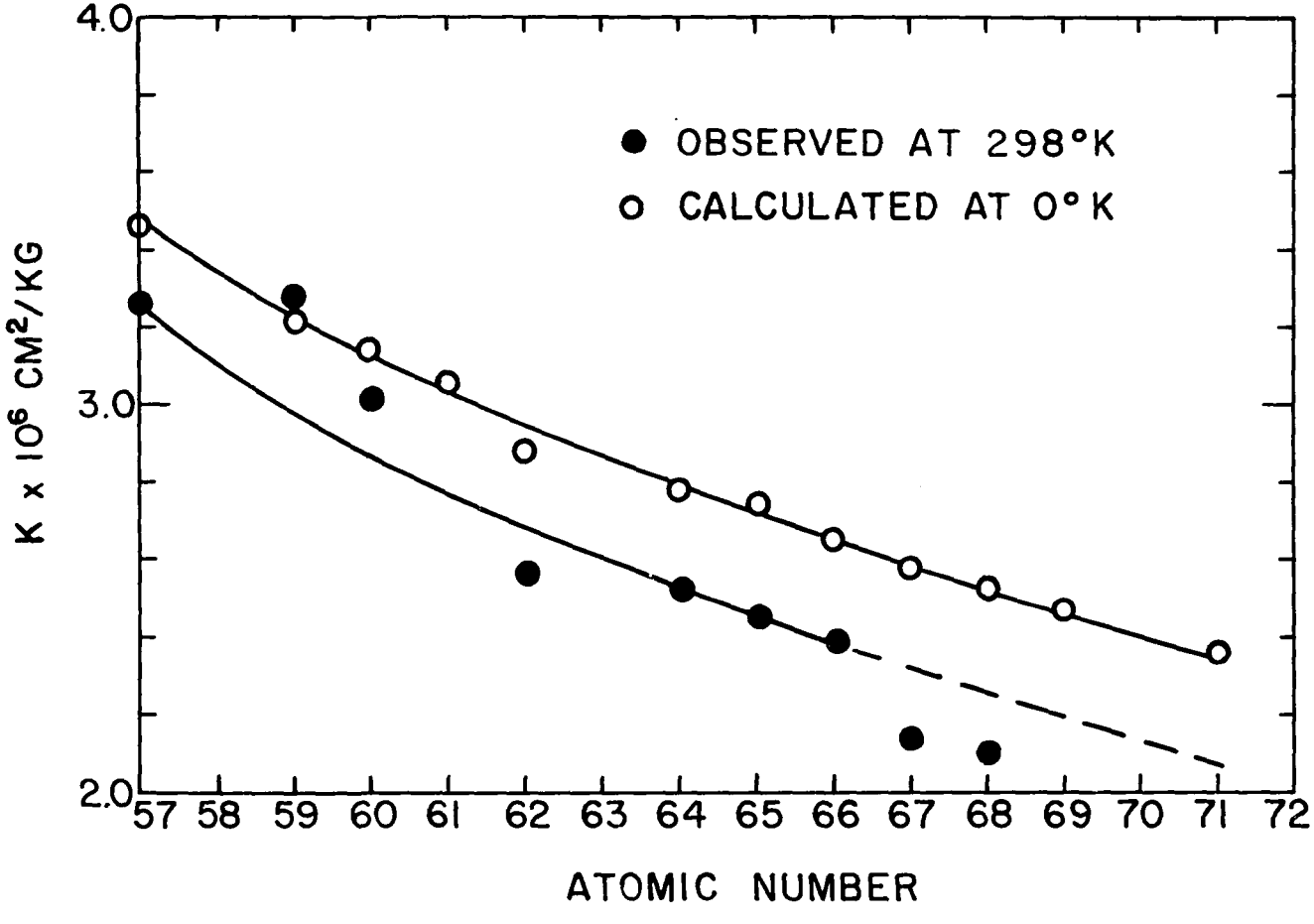
4.0
3.0
2.0
K x 10⁶ CM²/KG
● OBSERVED AT 298°K
○ CALCULATED AT 0°K
57 58 59 60 61 62 63 64 65 66 67 68 69 70 71 72
ATOMIC NUMBER

IV. CALCULATION OF THE ELASTIC SHEAR CONSTANTS

A. General Considerations

It is convenient to divide the total energy E of a metal lattice in the following way:

$$E = E_o + E_F + E_{ex.} + E_{corr.} + E_I + E_L. \tag{63}$$

Equation 63 is just equation 32 rewritten in a qualitative fashion for ease of explanation. E_o is the energy of the lowest electronic state consisting of the sum of the kinetic energy of the lowest state, the potential energy due to the interaction of an ion with the negative charge inside an atomic sphere of radius r_s, and the self-potential energy of the valence electron charge distribution within an atomic sphere. E_o depends only on r_s and is thus a function of the volume only. E_F denotes the mean Fermi energy of the valence electrons. For monovalent metals the Fermi surface is approximately a sphere lying wholly within the first Brillouin zone and the Fermi energy depends only on the atomic volume. For polyvalent metals the effect of discontinuities at the zone boundaries due to the occupation of higher electronic states must be taken into account. The Fermi energy is strongly dependent upon the geometry of the Brillouin zone for polyvalent metals. The exchange and correlation energies, denoted by $E_{ex.}$ and $E_{corr.}$ respectively,

in equation 63 are a function only of atomic volume for free electrons. For polyvalent metals the exchange and correlation energies, like the Fermi energy, depend on the Brillouin zone structure. The non-Coulomb repulsive interaction of the ion-cores E_I is due to the overlapping of core shells and is dependent upon the atomic volume and the crystal structure. The final term in equation 63 is due to the non-spherical part of the charge distribution. E_L depends upon the volume and the crystal structure.

When a monovalent metal is sheared at constant volume there are two important contributions (6) to the elastic shear constants: (a) a purely electrostatic term arising from E_L representing the difference between the electrostatic energy of the ion-cores in the strained and unstrained geometry, and (b) a term arising from E_I due to the change in the short-range repulsive interactions of the core electrons. For polyvalent metals two additional terms arise from the Fermi energy and from the exchange and correlation energies. The Fermi, exchange and correlation terms are due to the shear distortion of the Brillouin zone. It is extremely difficult to make any estimate of the contribution of the exchange and correlation energies to the elastic shear constants, and these terms are neglected in the first approximation.

B. The Elastic Shear Strain Energy

For a hexagonal crystal there are three volume-conserving strains which may be taken as pure shears. C corresponds to a shear which changes the c/a ratio at constant volume and leaves the symmetry of the crystal unchanged. The shear corresponding to C is shown in Figure 3A. C' corresponds to a shear which changes the angle between any pair of orthogonal axes in the basal plane of the crystal leaving the c axis unaffected. The shear corresponding to C' is shown in Figure 3B. C" corresponds to a shear which tilts the c axis with respect to the basal plane. The shear corresponding to C" is shown in Figure 3C. The relations between the shear constants C, C', and C" and the ordinary elastic constants are shown in the following paragraphs.

Consider a shear corresponding to C. The sheared hexagonal close-packed lattice can be expressed by the lattice vectors

$$\hat{a}_1 = a/A(1,0,0),$$

$$\hat{a}_2 = a/A(-\tfrac{1}{2}, \sqrt{3}/2, 0),$$

$$\hat{a}_3 = c/A(0,0,1/\xi).$$

In order to fulfill the condition of constant volume during a finite strain $A^3 = 1/\xi$. At the equilibrium position $\xi = 1$. The displacement vector $\hat{\tau}$ is expressed as

Figure 3. Volume-conserving strains of a hexagonal crystal

A. Shear corresponding to C
B. Shear corresponding to C'
C. Shear corresponding to C"

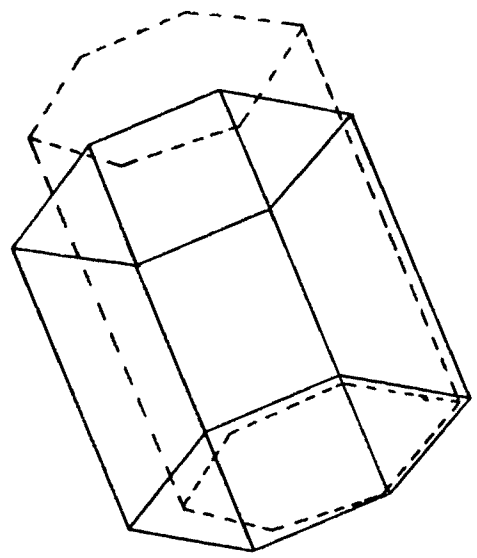

A

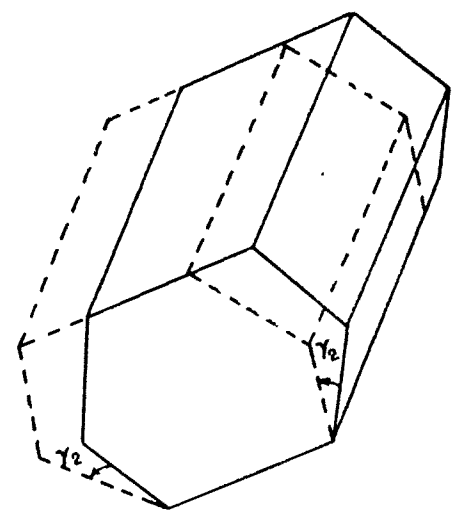

B

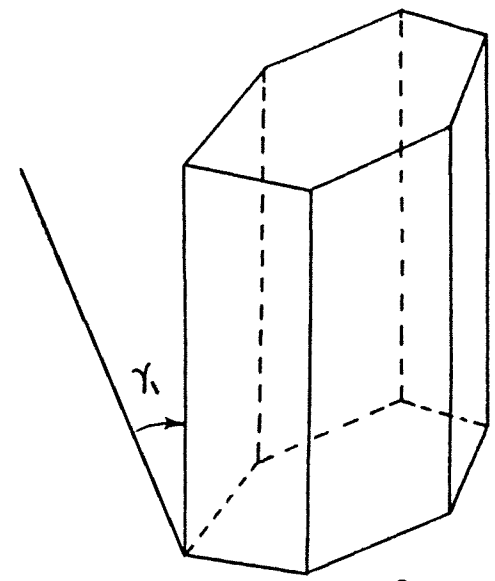

C

$$\hat{\tau} = \hat{r} \cdot (e), \tag{64}$$

where $\hat{r}$ is the initial position vector and (e) is the strain tensor. For a general point with position vector $\hat{r}$, the position vector $\hat{r}'$ after displacement is given by

$$\hat{r}' = \hat{r} + \hat{\tau} \ . \tag{65}$$

The components of (e) are obtained in terms of the strain parameter ξ by use of the lattice vectors for the strained and unstrained geometry and equations 64 and 65. The components of the strain tensor (e) for the shear corresponding to C are:

$$e_1 = e_2 = (A - 1),$$

$$e_3 = (\xi/A) - 1 \ ,$$

$$e_4 = e_5 = e_6 = 0.$$

The elastic strain energy of a hexagonal crystal can be written in terms of the five independent elastic constants and the components of the strain tensor. This relation is:

$$W = W_o + \tfrac{1}{2}c_{11}(e_1^2 + e_2^2) + \tfrac{1}{2}c_{33}e_3^2 + c_{12}e_1e_2 + c_{13}(e_1e_3 + e_2e_3) + \tfrac{1}{2}c_{44}(e_4^2 + e_5^2) + \tfrac{1}{4}(c_{11}-c_{12})e_6^2, \tag{66}$$

where e_1, e_2, and e_3 are the normal strains and $\frac{1}{2}e_4$, $\frac{1}{2}e_5$, $\frac{1}{2}e_6$ are the shear strains. The shear constant C is derived as

$$C = 9/2\ (d^2W/d\xi^2)_{\xi=1} = c_{11} + c_{12} + 2c_{33} - 4c_{13} \qquad (67)$$

by substitution of the appropriate values of e into equation 66 and differentiation with respect to the strain parameter. The shear strain ξ reflects a change in the reciprocal lattice which can be represented by the vectors $\hat{b}_j$ as:

$$\hat{b}_1 = 2\pi A/a(1, -1/\sqrt{3}, 0),$$

$$\hat{b}_2 = 2\pi A/a(0, 2/\sqrt{3}, 0),$$

$$\hat{b}_3 = 2\pi A/c(0, 0, \xi).$$

For C' the direct and reciprocal lattice vectors can be written (8) in terms of a strain parameter η as:

$$\hat{a}_1 = a\eta^{\frac{1}{2}}(1,0,0),$$

$$\hat{a}_2 = a\eta^{\frac{1}{2}}(-\tfrac{1}{2}, \sqrt{3}/2\eta, 0),$$

$$\hat{a}_3 = c(0,0,1),$$

$$\hat{b}_1 = 2\pi\eta^{-\frac{1}{2}}/a\ (1/\eta, 1/\sqrt{3}, 0),$$

$$\hat{b}_2 = 2\pi\eta^{-\frac{1}{2}}/a\ (0, 2/\sqrt{3}, 0),$$

$$\hat{b}_3 = 2\pi/c\ (0,0,1).$$

This strain results in the following relationship between C'

and the ordinary elastic constants:

$$C' = (d^2W/d\eta^2)_{\eta=1} = \tfrac{1}{2}(c_{11} - c_{12}). \tag{68}$$

Corresponding relationships for C" can be written (8) in terms of a strain parameter ϵ as:

$$\hat{a}_1 = a(1,0,\epsilon),$$

$$\hat{a}_2 = a(-\tfrac{1}{2}, \sqrt{3}/2, -\tfrac{1}{2}\epsilon),$$

$$\hat{a}_3 = c(0,0,1),$$

$$\hat{b}_1 = 2\pi/a(1,1/\sqrt{3},0),$$

$$\hat{b}_2 = 2\pi/a(0,2/\sqrt{3},0),$$

$$\hat{b}_3 = 2\pi/c(-\epsilon,0,1),$$

and

$$C'' = (d^2W/d\epsilon^2)_{\epsilon=0} = c_{44}. \tag{69}$$

Since the crystal is under no external stress at zero strain the condition for equilibrium is

$$(dW/dx)_o = 0, \tag{70}$$

where W is the elastic strain energy of equation 66 and x stands for one of the strain parameters ξ, η, or ϵ. The subscript zero implies the value at the equilibrium position.

Equation 70 must be obeyed by the total strain energy and is not necessarily valid for the individual contributing terms.

C. The Electrostatic Energy of the Lattice

The non-spherical part of the electronic charge distribution is represented in equation 63 by E_L. E_L is equal (19) to the difference between the energy E_1 of a lattice with positive point charges embedded in a uniform negative charge distribution and the energy E_s of a uniform spherical charge distribution within an atomic sphere of radius r_s. E_s depends on r_s and therefore changes with atomic volume only. For a volume conserving strain there is no contribution by E_s to the elastic constants.

By an extension of Ewald's method (35) for calculating the electrostatic energy of a lattice Fuchs (7) has expressed E_1 in the form:

$$E_1 = \frac{(e)^2}{2}\left\{\frac{1}{\pi\Omega}\sum_1{}' \frac{\exp - \frac{\pi^2}{E^2}h_1^2}{h_1^2} + \sum_1{}' \frac{1 - \phi(ER_1)}{R_1}\right.$$

$$\left. - \frac{\pi}{E^2\Omega} - \frac{2E}{\sqrt{\pi}}\right\} \qquad (71)$$

where

$$\phi(x) = \frac{2}{\sqrt{\pi}}\int_0^x \exp - t^2 dt, \text{ the normal probability}$$

integral,

R_l = lattice vector joining any two points in the lattice,

e = charge of an electron in esu,

h_l = vector of the reciprocal lattice,

Ω = atomic volume,

E = arbitrary parameter of the dimensions of reciprocal length to cause rapid convergence of the series.

The dash on the summation sign indicates that the terms where $h_l = 0$, $R_l = 0$, respectively, are to be excluded. The second derivative of E_l with respect to a strain parameter x is

$$\left(\frac{d^2E_l}{dx^2}\right)_o = \frac{e^2}{2\pi\Omega} \sum_l{}' \exp\frac{-\pi^2}{E^2} h_l^2 \left[\left(\frac{\pi^4}{E^4}\frac{1}{h_l^2} + \frac{2\pi^2}{E^2}\frac{1}{h_l^4} + \frac{2}{h_l^6}\right)\left(\frac{dh_l^2}{dx}\right)^2 - \left(\frac{\pi^2}{E^2}\frac{1}{h_l^2} + \frac{1}{h_l^4}\right)\frac{d^2h_l^2}{dx^2}\right]$$

$$+ \frac{e^2}{2}\left[\sum_l{}' \frac{2\exp(-E^2R_l^2)}{\sqrt{\pi}}\left\{\left(2E^3 + \frac{2E}{R_l^2}\right)\left(\frac{dR_l}{dx}\right)^2 - \frac{E}{R_l}\left(\frac{d^2R_l}{dx^2}\right)\right\} + \frac{1-\phi(ER_l)}{R_l^2}\left\{\frac{2}{R_l}\left(\frac{dR_l}{dx}\right)^2 - \frac{d^2R_l}{dx^2}\right\}\right]. \tag{72}$$

There are two complications that enter when E_l is considered for an actual metal; namely, (a) the original non-uniformity of the actual electron distribution, and (b) the

additional modulation of the electron distribution caused by the elastic distortion of the lattice, which tends to lower the associated strain energy. If one assumes that the electron distribution is spherically symmetric within an atomic sphere representing a cellular polyhedron and elsewhere constant, the first effect can be accounted for by multiplying E_1 by $(\nu_{eff})^2$ where (ν_{eff}) is ratio of the charge density at the cell boundary to its average value throughout the cell. On this basis Leigh (7) has suggested that the charge $(e)^2$ in equations 71 and 72 be replaced by $(\nu_{eff}e)^2$ with

$$\nu_{eff} = \Omega\left[\left\{\nu u_o^2(r_s)\right\}^2 - \left\{\nu u_o^2(r_s) - \rho(r_s)\right\}^2\right]^{\frac{1}{2}}. \tag{73}$$

In equation 73 ν is the ionic charge, $u_o = N\phi_o$ is the wave function for the state of lowest energy normalized over a single atomic cell, Ω is the atomic volume, and ρ the electron density. Raimes (18) has shown that in divalent magnesium $u_o^2(r_s)$ is almost equal to the average value of $u_o^2(r)$. If this result holds true for polyvalent metals in general, equation 73 takes the form

$$\nu_{eff} = \Omega\left[\nu^2 - \left\{\nu - \rho(r_s)\right\}^2\right]^{\frac{1}{2}}. \tag{74}$$

For the case of a perfectly uniform electron distribution

$\Sigma\Omega\rho(r_s)$ is equal to $\mathcal{N}$ and $\mathcal{N}_{eff} = \mathcal{N}$.

The influence of the second complication, the change in the spatial distribution of the electrons when the lattice is sheared at constant volume, can be treated in terms of the energies of the higher electronic states. Occupied states near the zone boundary are strongly affected by the distortion, and tend to reduce the electrostatic contribution to the elastic shear constants. Reitz and Smith (8) have postulated that the combined effect of non-uniform electron density, the change in the spatial distribution of the electrons during distortion, and electron relaxation effects will be such as to reduce the electrostatic contributions to the elastic shear constants of polyvalent metals to about one-half the maximum value. The values of the derivatives of R_1 and h_1 needed to solve equation 72 for a hexagonal close-packed metal under shear strains C, C', and C'' are given in Appendix A.

D. The Non-Coulomb Repulsive Interactions of the Ion-Cores

The non-Coulomb repulsive interaction energy of the ion-cores is represented in equation 63 by E_I. The energy E_I per atom is

$$E_I = \tfrac{1}{2} \sum_R W_R. \qquad (75)$$

The second derivative of E_I with respect to a strain parameter is

$$\frac{(d^2E_I)}{dx^2} = \tfrac{1}{2} \sum_{R_1} \frac{(dR_1)}{dx} \frac{(d^2W_R)}{dx^2} + \frac{(d^2R_1)}{dx^2} \frac{(dW_R)}{dx} . \qquad (76)$$

For metals in which the clearance between ion-cores is relatively large the interaction potential W_R can be represented (19) as:

$$W_R = Ab \exp \left[2r_c - R_1/\rho \right] . \qquad (77)$$

The symbol A represents the dependence of the repulsive potential upon the charge of the ions and is 1.75 for a trivalent ion. The distance between two ions is represented by R_1 and the ionic radius by r_c. The constants b and ρ are determined empirically from the lattice constant and compressibility and are equal to 10^{-12} erg and 0.3×10^{-8} cm, respectively, for most elements.

E. The Fermi Energy

The Brillouin zone of a polyvalent hexagonal close-packed metal is shown in Figure 4. There are three valence electrons per atom for scandium, yttrium, and the trivalent rare earth metals. The Brillouin zone contains sufficient states for exactly two valence electrons per atom. The remaining valence electron occupies states overlapping the boundary planes of the zone. Three possibilities exist as to the position of electron overlap: (a) B overlap across the faces perpendicular to the c axis defined by the $\{ 000,2 \}$ planes, (b) P overlap across the faces defined by the $\{ 1\bar{1}0,1 \}$ planes, and (c) Q

Figure 4. The Brillouin zone of a hexagonal close-packed metal showing the positions of electron overlap and holes

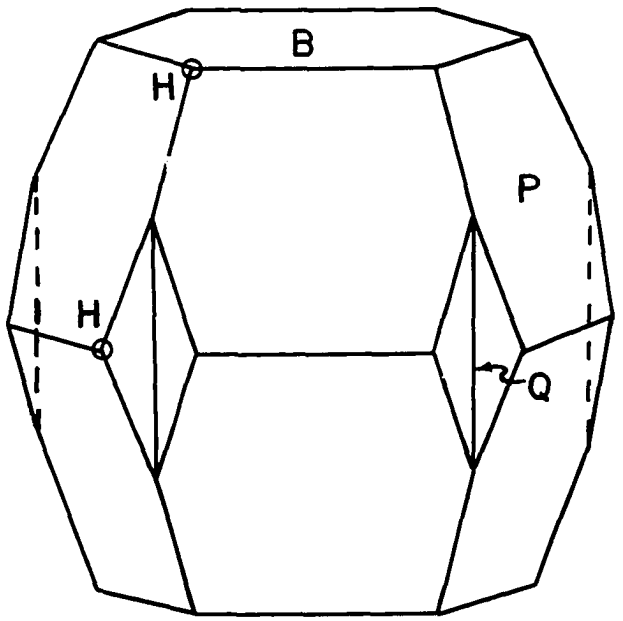
B
H
P
H
Q

overlap across the faces defined by the $\{1\bar{1}0,0\}$ planes. If the Brillouin zone is not full there are holes in the zone and an increased number of overlap electrons. The position of the holes in the Brillouin zone are marked by the symbol H in Figure 4.

The contribution of the Fermi energy to the elastic shear constants arises from electrons of wave-number not equal to zero. The lack of information concerning the nature of the energy surfaces for the rare earths and related metals necessitates some simple assumptions consistent with the nearly-free electron theory of metals in order to evaluate the contribution of the Fermi energy to the elastic shear constants. Following Leigh (7) the Fermi energy is broken up into two parts, (a) a contribution to the Fermi energy based upon the assumption of a completely filled Brillouin zone (W_F^I), and (b) a contribution from overlapping electrons and holes (W_F^{II}). The overlap-hole term compensates for the neglect of holes in the full zone term by assigning a negative value to the energies of the holes. The contribution to the elastic shear constants from a completely filled Brillouin zone arises from the energy changes which accompany distortion and are due to the shift of the Brillouin zone boundaries. The overlap-hole contribution to the elastic shear constants arises from the fact that strain distortion causes a displacement of the Fermi surface; this displacement is accompanied by a simultaneous transfer of electrons from

one overlap position to another.

By dividing the Brillouin zone into tetrahedra as proposed by Leigh (7) the full zone contribution to the elastic shear constants may be calculated. One such tetrahedron is shown in Figure 5. The vertices of the tetrahedron are the origin 0, the symmetrical center P of a face (which even in the strained zone is the point at which the face is met by the perpendicular from the origin), a corner point R of the face, and the foot Q of the perpendicular from P to an edge of the face adjacent to R. As suggested by Leigh (7) the one-electron energy is approximated by

$$E(\hat{k}) = \alpha_o(\hbar^2/2m)\left[k^2 - \lambda\left\{p^2(k_z/p)^{2/\lambda} + q^2(k_y/q)^{2/\lambda} + r^2(k_x/r)^{2/\lambda}\right\}\right], \quad (79)$$

where k_z, k_y, k_x are measured along p, q, and r, respectively, and α_o is the inverse effective mass ratio (m/m^*) for the center of the Brillouin zone. The parameter λ varies between 0 and 1.0 and is chosen so that $(dE(\hat{k})/dk)$ is zero at the zone boundaries. The contribution to the Fermi energy by each tetrahedron, obtained from equation 79, is:

$$(W_F^I)_{tet.} = (\alpha_o/4\pi^3)(\hbar^2/2m)(pqr/10)\left[F_p^2 + Gq^2 + Hr^2\right], \quad (80)$$

where

Figure 5. View of part of the Brillouin zone showing one of the tetrahedra used to compute the full-zone energy

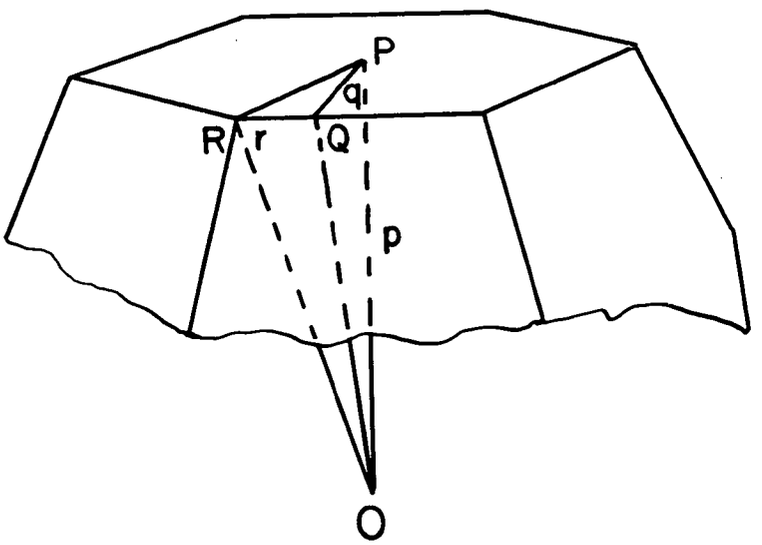
P
q
R
r
Q
p
O

$$F = 1 - 5\lambda^2/(2 + 3\lambda),$$

$$G = 0.5 - 5\lambda^3/(2 + 3\lambda)(1 + \lambda),$$

$$H = 1/6 - 5\lambda^4/(2 + 3\lambda)(1 + \lambda)(2 + \lambda).$$

The first and second derivatives of the full zone energy are fairly insensitive to the value of λ (7). On this basis the actual values calculated for the full zone contribution are those for $\lambda = 0$. Since p, q, and r are related to the reciprocal lattice vectors the contribution of a completely filled Brillouin zone to the elastic shear constants may be obtained by differentiation of equation 80.

In a calculation of the elastic shear constants of magnesium Reitz and Smith (8) calculated the full zone contributions to the elastic shear constants C and C'. Seven different tetrahedra were required for calculating the full zone contribution to C and eighteen different tetrahedra for C'. The full zone contribution to C" was not computed due to the low symmetry of the shear distortion. The values of p, q, and r for the Brillouin zone of a polyvalent hexagonal close-packed metal for the shears corresponding to C and C' are given in terms of the a/c ratio in Tables 7 and 8 respectively. The full zone contributions to C and C' for a hexagonal close-packed metal are given in Appendices B and C respectively. The full zone contribution to C" was not computed.

Table 7

Values of p, q, and r for the Brillouin zone of a hexagonal close-packed metal under a shear corresponding to C

Tetrahedron	Face	Quantity
1	B	$p_1 = \frac{2\pi}{a}\xi^{-1/3}(a/c)\xi$
		$q_1 = \frac{2\pi}{a\sqrt{3}}\xi^{-1/3}(1 - 3/4(a/c)^2\xi^2)$
		$r_1 = \frac{2\pi}{3a}\xi^{-1/3}(1 - 3/4(a/c)^2\xi^2)$
2	P	$p_2 = \frac{2\pi}{a\sqrt{3}}\xi^{-1/3}(1 + 3/4(a/c)^2\xi^2)^{\frac{1}{2}}$
		$q_2 = \frac{\pi}{a}\xi^{-1/3}(a/c)(1 + 3/4(a/c)^2\xi^2)^{\frac{1}{2}}$
		$r_2 = r_1$
3	P	$p_3 = p_2$
		$q_3 = \frac{2\pi}{3a}\xi^{-1/3}\frac{(1 + 3/4(a/c)^2\xi^2)^{\frac{1}{2}}}{(1 + (a/c)^2\xi^2)^{\frac{1}{2}}}$
		$r_3 = \frac{\pi}{3a}\xi^{-1/3}\frac{\xi}{(1 + (a/c)^2\xi^2)^{\frac{1}{2}}}$
4	P	$p_4 = p_3$

Table 7. (Continued)

Tetrahedron	Face	Quantity
4	P	$q_4 = q_3$
		$r_4 = \frac{2\pi\xi^{-1/3}}{3a}(a/c)\frac{(1 + 3/2(a/c)^2\xi^2)^{\frac{1}{2}}}{(1 + (a/c)^2\xi^2)^{\frac{1}{2}}}$
5	Q	$p_5 = \frac{2\pi\xi^{-1/3}}{a\sqrt{3}}$
		$q_5 = \frac{2\pi\xi^{-1/3}}{3a}$
		$r_5 = \frac{\pi\xi^{-1/3}}{a}(a/c)\xi$
6	Q	$p_6 = p_5$
		$q_6 = \frac{2\pi\xi^{-1/3}}{3a}\frac{(1+3(a/c)^2\xi^2+9/4(a/c)^4\xi^4)^{\frac{1}{2}}}{(1+a/c)^2\xi^2)^{\frac{1}{2}}}$
		$r_6 = r_3$
7	Q	$p_7 = p_5$
		$q_7 = q_6$
		$r_7 = 4_4$

Table 8

Values of p, q, and r for the Brillouin zone of a hexagonal close-packed metal under a shear corresponding to C'

Tetrahedron	Face	Quantity
1	B	$p_1 = \frac{2\pi}{a}(a/c)$
		$q_1 = \frac{2\pi}{a\sqrt{3}}\eta^{\frac{1}{2}}(1 - 3/4\eta\,(a/c)^2)$
		$r_1 = \frac{\pi}{a}\eta^{-\frac{1}{2}}(1 - \eta\,2/3 - \frac{1}{2}(a/c)^2\eta)$
2	B	$p_2 = p_1$
		$q_2 = \frac{\pi}{a}\eta^{-\frac{1}{2}}(1 + \eta 2/3)^{\frac{1}{2}}$ $\left(1 - (a/c)^2\eta/(1 + \frac{\eta^2}{3})\right)$
		$r_3 = \frac{\pi}{a\sqrt{3}}\eta^{\frac{1}{2}}(1 + \eta\,2/3)^{\frac{1}{2}}$ $\left(1 - (a/c)^2\,\frac{(3 - \eta^2)}{2\eta(1 + \eta\,2/3)}\right)$
3	B	$p_3 = p_1$
		$q_3 = q_2$

Table 8. (Continued)

Tetrahedron	Face	Quantity
3	B	$r_3 = \frac{\pi}{a\sqrt{3}} \eta^{\frac{1}{2}}(1 + \eta 2/3)^{\frac{1}{2}} \left(1 - (a/c)^2 \frac{\eta}{(1 + \eta 2/3)}\right)$
4	P	$p_4 = \frac{2\pi}{a\sqrt{3}} \eta^{\frac{1}{2}} \left(1 + \frac{3}{4\eta}(a/c)^2\right)^{\frac{1}{2}}$
		$q_4 = \frac{\pi}{a}(a/c)\left(1 + \frac{3}{4\eta}(a/c)^2\right)^{\frac{1}{2}}$
		$r_4 = r_1$
5	P	$p_5 = \frac{\pi}{a}\left(\frac{(1 + \eta 2/3)}{\eta} + (a/c)^2\right)^{\frac{1}{2}}$
		$q_5 = \frac{\pi}{a}(a/c)\left(1 + (a/c)^2 \frac{\eta}{(1 + \eta 2/3)}\right)^{\frac{1}{2}}$
		$r_5 = r_2$
6	P	$p_6 = p_5$
		$q_6 = q_5$
		$r_6 = r_3$

Table 8. (Continued)

Tetrahedron	Face	Quantity
7	P	$p_7 = p_4$
		$q_7 = \frac{\pi}{a}\eta^{-\frac{1}{2}} \frac{(1-\eta 2/3)\left(1+3/4\eta\,(a/c)^2\right)^{\frac{1}{2}}}{\left(1+3/4\eta\,(a/c)^2(1+\eta 2/3)\right)^{\frac{1}{2}}}$
		$r_7 = \frac{\pi}{2a}(a/c) \frac{(1-\eta 2/3)}{\left(1+3/4\eta\,(a/c)^2(1+\eta 2/3)\right)^{\frac{1}{2}}}$
8	P	$p_8 = p_5$
		$q_8 = \frac{\pi}{a\sqrt{3}}\eta^{\frac{1}{2}} \frac{\left((1+\eta 2/3)+\eta\,(a/c)^2\right)^{\frac{1}{2}}}{\left(1+3/4\eta\,(a/c)^2(1+\eta 2/3)\right)^{\frac{1}{2}}}$
		$r_8 = r_7$
9	P	$p_9 = p_4$
		$q_9 = q_7$
		$r_9 = \frac{\pi}{2a}(a/c) \frac{(1+\eta 2/3)\left(1+3/2\eta\,(a/c)^2\right)}{\left(1+3/4\eta\,(a/c)^2(1+\eta 2/3)\right)^{\frac{1}{2}}}$
10	P	$p_{10} = p_5$
		$q_{10} = q_8$

Table 8. (Continued)

Tetrahedron	Face	Quantity
10	P	$r_{10} = r_8$
11	P	$p_{11} = p_5$
		$q_{11} = \frac{\pi}{a\sqrt{3}} \eta^{\frac{1}{2}} \frac{\left((1+\eta 2/3) + (a/c)^2 \eta\right)^{\frac{1}{2}}}{\left(1+(a/c)^2 \eta\right)^{\frac{1}{2}}}$
		$r_{11} = \frac{\pi}{3a}(a/c) \frac{\eta^2}{\left(1+(a/c)^2 \eta\right)^{\frac{1}{2}}}$
12	P	$p_{12} = p_5$
		$q_{12} = q_{11}$
		$r_{12} = \frac{\pi}{a}(a/c) \frac{\left(1-1/3\,\eta^2+(a/c)^2 \eta\right)}{\left(1+(a/c)^2 \eta\right)^{\frac{1}{2}}}$
13	Q	$p_{13} = \frac{\pi}{a} \eta^{-\frac{1}{2}} (1 + \frac{\eta^2}{3})^{\frac{1}{2}}$
		$q_{13} = \frac{\pi}{a\sqrt{3}} \eta^{\frac{1}{2}} (1 + \eta 2/3)^{\frac{1}{2}}$
		$r_{13} = \frac{\pi}{a} (a/c)$
14	Q	$p_{14} = p_{13}$

Table 8. (Continued)

Tetrahedron	Face	Quantity
14	Q	$q_{14} = \frac{\Pi}{a} \frac{\left[(1+\eta 2/3)^2\left(\frac{1}{3}\eta + (a/c)^2 + \frac{3}{4\eta}(\frac{a}{c})^4\right)\right]^{\frac{1}{2}}}{\left(1 + \frac{3}{4\eta}(a/c)^2 (1 + \eta 2/3)\right)^{\frac{1}{2}}}$
		$r_{14} = r_7$
15	Q	$p_{15} = p_{13}$
		$q_{15} = q_{14}$
		$r_{15} = r_9$
16	Q	$p_{16} = \frac{2\Pi}{a\sqrt{3}} \eta^{\frac{1}{2}}$
		$q_{16} = \frac{\Pi}{a} \eta^{-\frac{1}{2}} (1 - \eta 2/3)$
		$r_{16} = r_{13}$
17	Q	$p_{17} = p_{16}$

Table 8. (Continued)

Tetrahedron	Face	Quantity
17	Q	$q_{17} = \frac{\pi}{a}\eta^{-\frac{1}{2}} \frac{\left[(1-\eta 2/3)^2+(\frac{c}{c})^2\eta\,(2-\frac{2}{3}\eta^2+(\frac{a}{c})^2\eta\,)\right]^{\frac{1}{2}}}{1+(a/c)^2}$
		$r_{17} = \frac{\pi}{a}(a/c)\,\frac{(1-\eta 2/3+(a/c)^2\eta)}{(1+(a/c)^2\eta)^{\frac{1}{2}}}$
18	Q	$p_{18} = p_{16}$
		$q_{18} = q_{16}$
		$r_{18} = r_{11}$

The overlap-hole contribution to the elastic constants arises from (a) the displacement of the Fermi surface during a shear at constant volume, and (b) the simultaneous electron transfer from those faces receding from the origin of the Brillouin zone to those approaching it. It follows from the symmetry of the reciprocal lattice that the perpendicular distances from the origin to opposite faces of the Brillouin zone are always equal. These can then be summed in pairs.

Retaining the same notation as Leigh the subscript i denotes the type of overlap (or hole), and j the number of pairs of each type. The density of states N(E) is defined as the number of states per unit energy range. The quantity $N_i(E-E_{ij})$ represents the contribution to N(E) from the pair of faces with energy E_{ij} at the center of a face. The total number of carriers in each pair is denoted by n_{ij}. The quantity n_{ij} is positive for electron overlap, and <u>negative</u> for holes. The derivative of the Fermi level $\mathcal{J}$ with respect to strain is given (8) by the relation

$$\left(\frac{d\mathcal{J}}{dx}\right)_o = \left[\sum_{ij} N_i(|\mathcal{J}-E_{ij}|)^{-1} \times \sum_{ij} N_i(|\mathcal{J}-E_{ij}|)\left(\frac{dE_{ij}}{dx}\right)_o\right]. \tag{81}$$

The first and second derivatives of the overlap-hole contribution to the Fermi energy with respect to strain are given (8) by

$$\left(\frac{dW_F^{II}}{dx}\right)_o = \sum_{ij} n_{ij}\left(\frac{dE_{ij}}{dx}\right)_o, \tag{82}$$

and

$$\left(\frac{d^2W_F^{II}}{dx^2}\right)_o = \left[\sum_{ij} n_{ij}\left(\frac{d^2E_{ij}}{dx^2}\right)_o\right.$$

$$+ \sum_{ij} N_i(|\mathcal{F} - E_{ij}|) \left\{ \left(\frac{d\mathcal{F}}{dx}\right)_o^2 - \left(\frac{dE_{ij}}{dx}\right)_o^2 \right\} \Bigg]. \quad (83)$$

In order to obtain numerical results for equations 82 and 83 it is assumed that the energies E_{ij} are proportional to the distance of the electron overlap position (or hole position) from the origin. The first and second derivatives of E_{ij} with respect to the strain are assumed proportional to E_{ij}, the constant of proportionality being determined uniquely by the geometry of the Brillouin zone. On the basis of the nearly-free electron model the electron overlap positions are approximated by spheroids. B overlap consists of one pair or one complete spheroid, P overlap six spheroids, and Q overlap two spheroids. If the holes are not too large they may also be approximated by spheroids. The holes make up six spheroids. It should be emphasized that approximation of the holes in the Brillouin zone by spheroids is consistent with inverted spherical energy surfaces for the holes as long as the number of holes is not too large.

On the basis of the assumption of spheroidal energy surfaces the number of overlapping electrons (or holes) of type i is given (7) by

$$n_i = \frac{\Omega}{3\pi^2} \frac{1}{\sqrt{\alpha_i}} \left[\frac{8\pi^2 m}{h^2} |(\mathcal{F}_o - E_i)| \right]^{3/2}, \quad (84)$$

where Ω is the atomic volume and α_i is the inverse effective

mass ratio (m/m^*) at the overlap or hole position. The density of electron (or hole) states of type i with spheroidal energy surfaces is given (7) by the relation

$$N_i = \frac{3}{2} \frac{n_i}{|\zeta_o - E_i|} \quad . \tag{85}$$

F. Results

The decomposition of the elastic shear constants at 0°K into an electrostatic term, a core-repulsion term, and a Fermi term provides a relationship from which one can infer something about the number and position of overlap electrons in a metal. A knowledge of the following parameters is necessary in order to evaluate the individual contributions to the elastic shear constants and the positions of electron overlap: (a) the measured values of C and C', (b) the density of states, N(E), at the Fermi level, (c) the inverse effective mass ratio, α_o, for the center of the Brillouin zone, (d) the energies, E_{ij}, of the overlap electrons and holes in the Brillouin zone, (e) the Fermi level, and (f) the electrostatic reduction factor.

The experimental values of C and C' at 4.2°K were available for yttrium (5). An estimated value of the density of states at the Fermi level in yttrium of 69.8×10^{33} erg^{-1}

cm^{-3} was obtained from Jennings* based upon specific heat measurements**. The values of α_o, the E_{ij}, and the Fermi level may be determined from the soft X-ray spectrum of an element. This information was not available for yttrium. Values of α_o, the E_{ij}, and the Fermi level were adjusted by simultaneously varying α_o and the electrostatic reduction factor in order to fit the measured values of C and C'.

In order to evaluate the various shear constants equation 70 must be valid for the total strain energy. At the observed c/a ratio of yttrium at 0°K (36) of 1.567

$$(dE_1/d\xi)_o = 58.5F \times 10^9 \text{ erg cm}^{-3},$$

$$(dE_I/d\xi)_o = 0.6 \times 10^9 \text{ erg cm}^{-3},$$

$$(dW_F^I/d\xi)_o = -6.9\alpha_o \times 10^9 \text{ erg cm}^{-3},$$

where F is the electrostatic reduction factor and α_o is the inverse effective mass ratio for the center of the zone. The relations for determining the individual contributions to $(dW/d\xi)_o$ are given in Appendix D. The overlap-hole contribution, $(dW_F^{II}/d\xi)_o$, depends upon the derivatives of the

---

*Jennings, L. D., Ames, Iowa. The specific heat of yttrium. Private communication. 1959.

**The value of N(E) was based upon the extrapolation of measurements of the specific heat at 12°K.

various E_{ij} with respect to the strain. These values for yttrium at 0°K are listed in Table 9. The condition that $(dW/d\xi)_o = 0$ was utilized to estimate the numerical value of $(dW_F^{II}/d\xi)_o$. Choosing α_o equal to one and the electrostatic reduction factor F equal to one-half (8) the derivative of the overlap-hole contribution with respect to the strain parameter was estimated as

$$(dW_F^{II}/d\xi)_o = -22.95 \times 10^9 \text{ erg cm}^{-3}. \qquad (86)$$

The interesting result is that the number in equation 86 is negative; hence, overlaps or holes with a negative $n_{ij}(dE_{ij}/d\xi)_o$ must be predominant in yttrium at 0°K. This result considered in light of the values in Table 9 shows that P and/or Q overlap must be predominant although B overlap may also be present. The result of equation 86 cannot be corroborated for the shear corresponding to C' since $(dE_1/d\eta)_o$, $(dE_I/d\eta)_o$, $(dW_F^I/d\eta)_o$, and $(dW_F^{II}/d\eta)_o$ are each identically zero for all c/a ratios (8).

If the nearly-free electron approximation is valid for yttrium, the inverse effective mass ratio, α_o, for the center of the Brillouin zone cannot differ very greatly from the free electron value of one. In addition the electrostatic reduction factor, F, cannot be much less (8) than one-half. At the observed c/a ratio of yttrium at 0°K (36) of 1.567

$$C_1 = 9/2\ (d^2E_\ell/d\xi^2)_o = 29.42F \times 10^{11} \text{ dynes/cm}^2,$$

Table 9

First and second derivatives of the various overlap and hole energies in yttrium at 0°K with respect to the shear parameters ξ and η

Type	Number of spheroids	$(\frac{dE_{ij}}{d\xi})_o$	$(\frac{dE_{ij}}{d\eta})_o$	$(\frac{d^2E_{ij}}{d\xi^2})_o$	$(\frac{d^2E_{ij}}{d\eta^2})_o$
P	2	$-0.2006\ E_P$	$0.7670\ E_P$	$0.9557\ E_P$	0
	2	$-0.2006\ E_P$	$-0.3835\ E_P$	$0.9557\ E_P$	$1.1505\ E_P$
	2	$-0.2006\ E_P$	$-0.3835\ E_P$	$0.9557\ E_P$	$1.1505\ E_P$
Q	2	$-(2/3)\ E_Q$	0	$(10/9)\ E_Q$	$(3/2)\ E_Q$
B	1	$(4/3)\ E_B$	0	$(4/9)\ E_B$	0
H	2	$0.0330\ E_H$	$0.0758\ E_H$	$1.4068\ E_H$	$1.2824\ E_H$
	2	$0.0330\ E_H$	$0.0758\ E_H$	$1.4068\ E_H$	$1.2824\ E_H$
	2	$0.0330\ E_H$	$-0.1515\ E_H$	$1.4068\ E_H$	$0.8568\ E_H$

$$C_I = 9/2(d^2E_I/d\xi^2)_o = 1.44 \times 10^{11}\ \text{dynes/cm}^2,$$

$$C_F^I = 9/2(d^2W_F^I/d\xi^2)_o = 11.21\alpha_o \times 10^{11}\ \text{dynes/cm}^2.$$

On the basis of the above values and the measured value of C (5) of 19.67×10^{11} dynes/cm^2 the overlap-hole contribution to C must be negative. As seen from equation 83 and Table 9, a negative overlap-hole contribution to C is due primarily to

B-type overlap. The individual contributions to C' from the electrostatic, core-repulsion, and full zone terms are:

$$C_1' = (d^2E/d\eta^2)_o = 5.120F \times 10^{11} \text{ dynes/cm}^2,$$

$$C_I' = (d^2E_I/d\eta^2)_o = 0.444 \times 10^{11} \text{ dynes/cm}^2,$$

$$C_F'^I = (d^2W_F^I/d\eta^2)_o = 1.815\alpha_o \times 10^{11} \text{ dynes/cm}^2.$$

On the basis of the above values and the measured value of C' (5) of 2.715×10^{11} dynes/cm^2 the overlap-hole contribution to C' must also be negative. Examination of equation 83 and Table 9 indicates that a negative overlap-hole contribution to C' is due to P-type overlap. In order to fit the measured values of C and C' at 0°K on the basis of only B and P overlaps an appreciable number of holes in the Brillouin zone must be assumed. The number of holes per atom in the Brillouin zone was obtained from the relation

$$6n_H = n_B + 6n_P - 1, \tag{87}$$

where n_H is the number of holes per atom associated with one of the six spheroids which approximate the holes, n_B is the total number of electrons per atom in B overlap positions, and n_P is the number of electrons per atom associated with one of the six spheroids of type P. The numerical values of n_B, $6n_P$, and $6n_H$ were obtained from the relations

$$N(E) = 1.5 \frac{n_B}{|\mathcal{J}_o - E_B|} + 9 \frac{n_P}{|\mathcal{J}_o - E_P|} + 9 \frac{n_H}{|\mathcal{J}_o - E_H|} \qquad (88)$$

and

$$(dW_F^{II}/d\xi)_o = 1.3333\ n_B E_P - 1.2036\ n_P E_P - 0.1980\ n_H E_H. \qquad (89)$$

The E_{ij} were modified by means of equation 79 so that (dE_{ij}/dk) was zero at the boundaries of the Brillouin zone. The value of α_o, and hence the E_{ij} and $\mathcal{J}_o$, were obtained by simultaneously varying α_o and the electrostatic reduction factor in order to obtain reasonable agreement with the measured values of C and C'. The quantities used in equations 83, 88, and 89 to determine the overlap hole contribution to the elastic shear constants are given in Table 10.

Table 10

Quantities used in equations 83, 88, and 89 to determine the overlap-hole contribution to the elastic shear constants

Quantity	Value
E_B	4.00 eV
E_P	3.35 eV
E_H	4.11 eV
$\mathcal{J}_o$	4.42 eV
α_o	0.7

Table 10. (Continued)

Quantity	Value
F	0.6
n_B	1.60×10^{21} cm^{-3}
$6n_P$	39.30×10^{21} cm^{-3}
$6n_H$	10.60×10^{21} cm^{-3}
N(E)	69.8×10^{33} erg^{-1}cm^{-3}
N_B	3.64×10^{33} erg^{-1}cm^{-3}
$6N_P$	34.27×10^{33} erg^{-1}cm^{-3}
$6N_H$	31.89×10^{33} erg^{-1}cm^{-3}

The calculated contribution of the individual terms to the elastic shear constants C and C' of yttrium at 0°K are given in Table 11.

Table 11

Contributions to the elastic shear constants of yttrium in units of 10^{11} dynes/cm^2 at 0°K

Term	C	C'
Electrostatic	17.65	3.072
Core repulsion	1.44	.444
Full zone	7.85	1.271

Table 11. (Continued)

Term	C	C'
Overlap-hole	-8.01	-2.257
Total	18.93	2.530
Experiment[a]	19.67	2.715

[a]Obtained from the experimental values of Smith and Gjevre (5).

It was not possible to obtain reasonable agreement with the measured values of C and C' by assuming (a) B and Q overlap and holes, or (b) P and Q overlap and holes. It was of interest to determine the effect of Q overlap, in addition to B and P overlaps and holes, upon the elastic shear constants. It was found that the assumption of more than approximately 0.2×10^{21} cm^{-3} Q overlap electrons made it impossible to obtain reasonable agreement with the measured values of C and C'. The qualitative result of this investigation is that B and P overlaps and holes have occurred in yttrium at $0^{\circ}K$ and any Q overlap that may be present must be small. The elastic shear constant C'' was not calculated due to the complexity of calculating the full zone contribution. A calculation of the elastic shear constants C and C' for scandium and the rare earth metals was not possible

since the single crystal elastic constants of these elements have not been measured.

As seen in Table 11, a value of α_o of 0.7 was assumed in order to obtain reasonable agreement with the observed elastic shear constants. In order to determine how the calculated atomic radius, compressibility, total energy, and cohesive energy of yttrium would be affected, an inverse effective mass ratio of 0.7 was substituted for the free electron value of 1.0 in calculating the mean Fermi energy of equation 46. The results are given in Table 12 in comparison to the observed quantities.

Table 12

Atomic radius, compressibility, total energy, and cohesive energy of yttrium

Atomic radius (Å)		Compressibility (x 10^6 cm^2/kg)		Total energy (kcal/mol)		Cohesive energy (kcal/mol)	
Calc.	Obs.	Calc.	Obs.	Calc.	Obs.	Calc.	Obs.
2.33[a]	1.99	2.69	2.31	944	1000	47	103
2.21[b]		2.38		1014		117	

[a]Obtained from Table 6.

[b]Calculated on the basis of $\alpha_o = 0.7$.

The shear modulus μ of a hexagonal metal may be represented in terms of the shear constants C, C', and C" by means of Voigt averaging (37). This relation is:

$$\mu = (1/30)\ (C + 12C' + 12C''). \tag{90}$$

The overlap-hole contribution to μ could not be calculated for the hexagonal rare earth metals due to the lack of the measured values of C, C', and C". In addition the contribution to C" from a completely filled Brillouin zone was not calculated because of the low symmetry of the distorted zone and the attendant complexity of the calculations. The maximum electrostatic and non-Coulomb core contributions to C, C', and C" were calculated in order to determine whether a general trend of increasing shear modulus with increasing atomic number would be shown. A second purpose was to evaluate how the neglect of the full zone and overlap-hole contributions to μ would affect the calculated dependence of the shear modulus on atomic number in comparison to the observed behavior (4). The maximum electrostatic contributions to C, C', and C", were calculated for the hexagonal rare earth metals by means of equation 72, the crystallographic information from Table 1, and the relations given in Appendix A. The contributions to C, C', and C" from the non-Coulomb core interactions were calculated from equations 76 and 77, the data from Tables 1 and 3, and the relations given in

Appendix A. The maximum electrostatic and non-Coulomb core contributions to C, C', C", and μ for the hexagonal rare earth metals are given in Table 13. The available experimental data (4) are listed for comparison. A plot of the calculated shear moduli of the hexagonal rare earth metals versus atomic number is shown in Figure 6 in comparison to the experimental behavior observed by Smith et. al. (4). Investigation of Figure 6 reveals that there is a general trend of increasing shear modulus with increasing atomic number for the calculated values although the dependence upon atomic number differs from the experimentally observed variation. On this basis one can surmise that the full zone and overlap-hole contributions to the shear moduli of the hexagonal rare earth metals must have quite a different dependence upon atomic number than the sum of the electrostatic, and non-Coulomb core contributions.

Table 13

Maximum electrostatic and non-Coulomb core contributions to C, C', C", and μ for the hexagonal rare earth metals in units of 10^{11} dynes/cm^2

Element	Atomic number	Maximum electrostatic contributions				Non-Coulomb core contributions				μ	
		C	C'	C"	μ	C	C'	C"	μ	Calc.	Obs.[a]
La	57	24.58	3.785	1.268	2.841	2.02	0.82	0.85	0.74	3.58	1.49
Pr	59	27.29	4.203	1.408	3.154	2.03	0.86	0.88	0.76	3.87	1.35
Nd	60	27.73	4.271	1.431	3.205	1.95	0.79	0.84	0.72	3.93	1.45
Sm	62	28.88	4.447	1.491	3.338	1.76	0.54	0.57	0.50	3.84	1.26
Gd	64	30.32	4.504	1.739	3.508	1.50	0.44	0.75	0.53	4.04	2.23
Tb	65	30.97	4.742	1.928	3.700	1.49	0.45	0.75	0.52	4.22	2.28
Dy	66	31.34	4.866	2.075	3.821	1.44	0.45	0.75	0.52	4.34	2.54
Ho	67	31.80	4.937	2.105	3.877	1.33	0.45	0.75	0.52	4.40	2.67
Er	68	32.47	5.041	2.149	3.958	1.34	0.42	0.73	0.50	4.46	2.96
Tm	69	33.25	5.163	2.201	4.042	1.34	0.42	0.73	0.50	4.54	--
Lu	71	34.90	5.263	2.086	4.103	1.34	0.42	0.73	0.50	4.60	--

[a]Experimentally determined by Smith et. al. (4).

Figure 6. Variation of the shear modulus with atomic number for the hexagonal rare earth metals

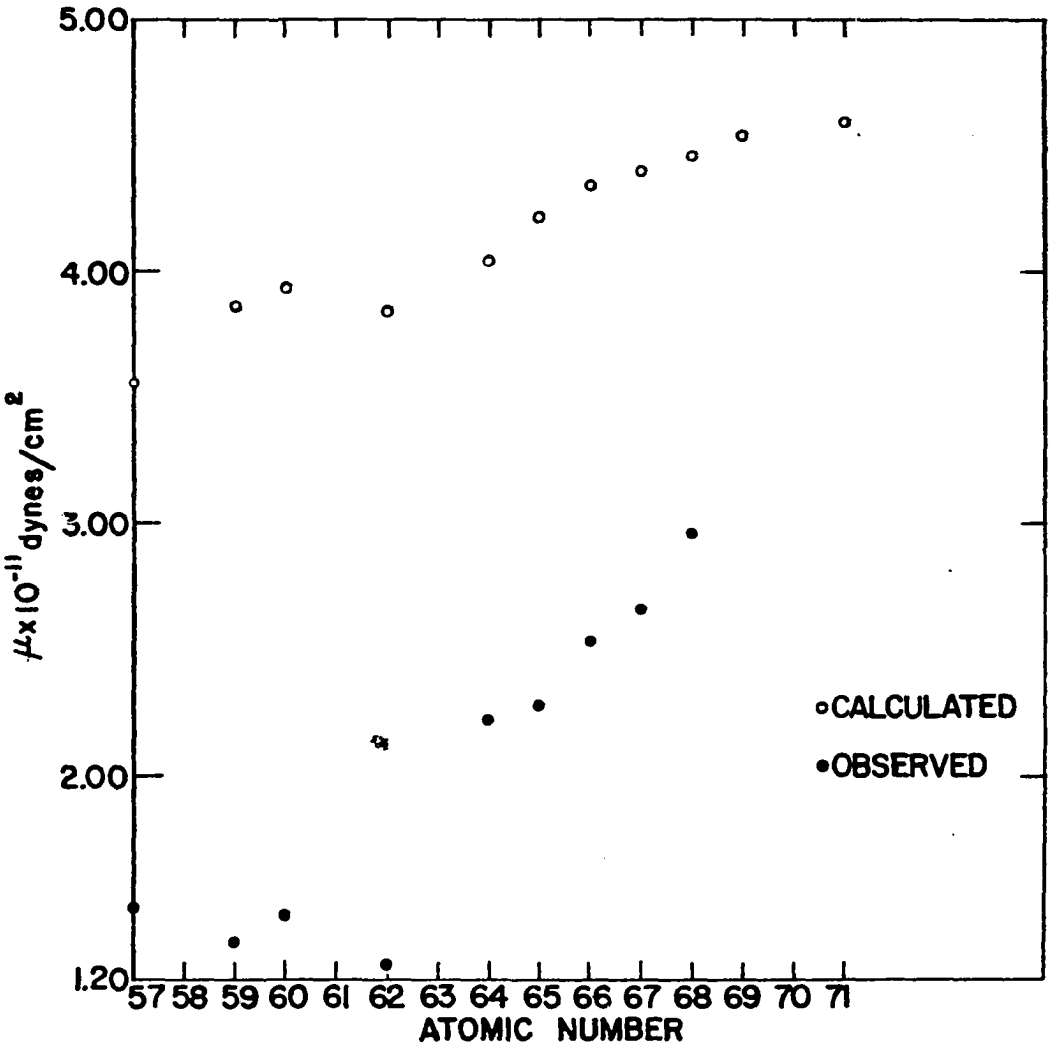
5.00
4.00
3.00
2.00
1.20
μx10⁻¹¹ dynes/cm²
57 58 59 60 61 62 63 64 65 66 67 68 69 70 71
ATOMIC NUMBER
○CALCULATED
●OBSERVED

V. DISCUSSION

The calculated results given in Table 6 show that the approximation of considering the valence electrons as free and sharing the same ground state wave functions is capable of giving fairly good agreement with experiment for the atomic radii and compressibilities of the hexagonal rare earths and related metals. In addition the calculated variation of atomic radius and compressibility with atomic number, shown respectively in Figures 1 and 2, is in qualitative agreement with the observed behavior of the hexagonal rare earth metals. The assumption of divalent behavior for europium and ytterbium gives fairly good agreement with experiment for these metals. The poor agreement between the calculated and observed results for cerium is not surprising as the approximation of treating all the valence electrons on an equivalent basis at zero wave number is poorest for this element. The calculated cohesive energy is the small difference between two large energies; one calculated on an approximate basis and the other empirical. Hence the poor agreement between the calculated and observed cohesive energies is to be expected. For this reason the total energies of the metals investigated have been tabulated in Table 6 and the correspondence between theory and experiment is here seen to be quite good.

The assumptions made in this investigation with regard to the ion-core potential would seem to be valid as a first approximation. The poor agreement between the screening number of the free scandium ion and the calculated value for the solid may be due to either or both of the following: (a) the assumption that the ion-cores remain unperturbed in going from the free neutral atom to the solid may not be valid for light elements such as scandium, or (b) the approximation of the ion-core radius in the metal by the empirical ionic radius in a salt may be poor for metals of low atomic number. It is interesting to note that almost the same value of r_o for europium, atomic number 63, was calculated independently by means of (a) the ionic crystal radius and (b) the empirical second ionization potential.

Probably the most questionable assumption of the modified cellular method of Raimes (9) is the neglect of the energy discontinuities at the zone boundaries and the treatment of the valence electrons as completely free. It might be noted that all the calculated quantities would be improved if the Fermi energy were slightly less than the free electron value. The results tabulated in Table 12 show that the use of an inverse effective mass ratio of 0.7 for yttrium was capable of greatly increasing the agreement between the calculated and observed quantities.

In consideration of the number and type of

approximations used in the modified cellular method for the rare earths and related metals the agreement with experiment is quite satisfactory. A possible explanation is that an appreciable amount of s-d hybridization is occurring in scandium, yttrium, and the rare earth metals due to the proximity of the first d level to the s ground level in the solid state. The occurrence of such hybridization would cause the assumption of equivalent behavior of the valence electrons for zero wave number to be particularly good. The possibility of compensating errors cannot be disregarded in any calculation of the type made in this investigation. This would be expected to have quite serious effects upon the magnitudes of the calculated atomic radii and compressibilities but it should be emphasized that this would not appreciably alter the good agreement between the calculated and experimental dependence of atomic radius and compressibility on atomic number for the hexagonal rare earth metals.

The qualitative result of the calculation of the elastic shear constants of yttrium is that B and P overlaps and holes are present at 0°K. As mentioned previously, the assumption was made that the valence electrons in yttrium share the same ground state wave functions and differ only in their wave-number vectors. This assumption implies that the first d level in yttrium lies quite close to the ground state at the center of the Brillouin zone. It is hence not unreasonable

to expect that near the zone boundaries the energies of some of the d levels may lie below the energy of the s level and an appreciable overlap occurs between the s and d bands in yttrium. The result of overlapping bands should lead to holes in the s band.

Additional support for the result of B and P overlaps and holes in yttrium comes from the theoretical calculation of the elastic shear constants of magnesium (8) by Reitz and Smith. In order to fit the measured values of C and C' for magnesium B and P overlaps and holes had to be assumed with B overlap predominant. The predominance of B overlap for magnesium is due to the nearly ideal c/a ratio (c/a = 1.6237) of this metal. Reitz and Smith (8) postulate that in zinc and cadmium the c/a ratios ($c/a \sim 1.8$) are so large that P overlap is prevented. Since the overlap-hole contribution to C' is due primarily to P-type overlaps the absence of P overlap in zinc and cadmium is the suggested reason for the large value of C' relative to C for these elements. On the basis of these arguments it would seem that as the c/a ratio becomes less than ideal P overlap increases and in the case of yttrium at $0^{\circ}K$ (c/a = 1.567) is predominant.

Probably the most questionable assumption made in the calculation of the overlap-hole contribution for yttrium is the assumption of inverted spherical energy surfaces for the holes. For a metal in which there are an appreciable number

of holes in the Brillouin zone the approximation of the energy surfaces of the holes by spheroids in calculating the change in the energy of the holes with respect to a strain parameter and the density of hole states is not strictly valid. In addition an approximate value was used for the total density of states at the Fermi level and necessary information from the soft X-ray spectrum of yttrium was not available. On the basis of the above discussion it is not possible at this time to attach great significance to the magnitudes of the calculated quantities given in Tables 10 and 11. It should be emphasized, however, that the qualitative result of electron overlap on the $\{000,2\}$ and $\{1\bar{1}0,1\}$ faces of the Brillouin zone and an appreciable number of holes in the zone is not expected to be in error if the nearly-free electron approximation is at all valid for yttrium.

Recently the electrical resistivities of single crystals of yttrium as a function of temperature (38) were measured. The results show that the resistivity in the basal plane is approximately two and one-quarter times as great as the resistivity along the c axis. It is interesting to interpret these results on the basis of the model proposed in this investigation for the position of overlap electrons in yttrium. If appreciable electron overlap has occurred across the $\{000,2\}$ faces of the Brillouin zone and little or no electron overlap has occurred in the equatorial plane of the zone then the total number of charge carriers (electrons +

holes) along the c axis of the crystal is greater than in the basal plane. If no electron overlap has occurred in the basal plane then the conduction in the basal plane of the crystal is purely by holes. The electrical resistivity of single crystals of yttrium would hence be expected to exhibit quite anisotropic behavior and this is indeed observed.

In conclusion it is suggested that experimental measurements of the lattice parameters and low temperature elastic constants of single crystals of yttrium as a function of electron to atom ratio would be of value in order to test the ideas proposed in this investigation. Variation of the electron to atom ratio could be achieved by a suitable choice of alloying materials. If no electron overlap is present in the equatorial plane of the Brillouin zone then the initiation of Q overlap should be reflected by a decrease in the c/a ratio with increasing electron to atom ratio. In addition the shear constant C should show an abrupt decrease at low temperatures upon the initiation of Q overlap with increasing electron to atom ratio of the type predicted by Reitz and Smith (8) for magnesium. Finally, it is hoped that experimental measurements of the soft X-ray spectrum and electronic specific heat of yttrium will provide the necessary information for a more accurate calculation of the contribution of the individual terms to the elastic shear constants and the number and density of overlap electrons and holes.

VI. LITERATURE CITED

1. Spedding, F. H., Legvold, S., Daane, A. H., and Jennings, L. D. Some physical properties of the rare earth metals. In Gorter, C. J., ed. Progress in low temperature physics. Vol. 2, pp. 368-394. New York, N. Y., Interscience Publishers, Inc. 1957.

2. Lawson, A. W. and Tang, T. Y. Phys. Rev. 76, 301 (1949).

3. Spedding, F. H., Daane, A. H., and Herrmann, K. W. Acta Cryst. 9, 559 (1956).

4. Smith, J. F., Carlson, C. E., and Spedding, F. H. J. Metals 9, 1212 (1957).

5. _____ and Gjevre, J. A. To be published in J. Appl. Phys. (1959).

6. Fuchs, K. Proc. Roy. Soc. (London) A153, 622 (1936).

7. Leigh, R. S. Phil. Mag. Ser. 7, 42, 139 (1951).

8. Reitz, J. R. and Smith, C. S. Phys. Rev. 104, 1253 (1956).

9. Raimes, S. Phil. Mag. Ser. 7, 43, 327 (1952).

10. Nye, J. F. Physical properties of crystals. London, Oxford University Press. 1959.

11. Love, A. E. H. A treatise on the mathematical theory of elasticity. 4th ed. New York, N. Y., Dover Publications, Inc. 1944.

12. Wigner, E. P. and Seitz, F. Phys. Rev. 43, 804 (1933).

13. Brooks, H. Suppl. Nuovo cimento 7, 165 (1958).

14. Lowdin, P. O. Phil. Mag. Suppl. 5, 1 (1956).

15. Reitz, J. R. Methods of the one-electron theory of solids. In Seitz, F. and Turnbull, D., eds. Solid state physics. Vol. 1, pp. 1-95. New York, N. Y., Academic Press, Inc. 1955.

16. Pines, D. Electron interactions in metals. In Seitz, F. and Turnbull, D., eds. Solid state physics.

Vol. 1, pp. 368-450. New York, N. Y., Academic Press, Inc. 1955.

17. Bloch, F. Z. Physik 52, 555 (1928).

18. Raimes, S. Phil. Mag. Ser. 7, 41, 568 (1950).

19. Seitz, F. Modern theory of solids. New York, N. Y., McGraw-Hill Book Co., Inc. 1940.

20. Raimes, S. Proc. Phys. Soc. (London) A66, 949 (1953).

21. Altmann, S. L. Proc. Roy. Soc. (London) A244, 153 (1958).

22. _____ and Cohan, N. V. Proc. Phys. Soc. (London) A71, 383 (1958).

23. Prokofjew, W. Z. Physik 58, 255 (1929).

24. Schiff, B. Proc. Phys. Soc. (London) A69, 185 (1956).

25. Templeton, D. H. and Dauben, C. H. J. Am. Chem. Soc. 76, 5237 (1954).

26. Moore, C. E. Atomic energy levels as derived from analysis of optical spectra. National Bureau of Standards. Circular 467 (Vol. 3). 1958.

27. Pauling, L. Nature of the chemical bond. 2nd ed. Ithaca, N. Y., Cornell University Press. 1940.

28. Sherman, J. Chem. Revs. 11, 93 (1932).

29. Bridgman, P. W. Proc. Am. Acad. Arts Sci. 83, 1 (1954).

30. Gschneidner, K. A., Jr. A compilation of the physical properties of the rare earth, scandium and yttrium metals. (Mimeo.) Los Alamos Scientific Laboratory, Los Alamos, New Mexico, Author. February, 1959.

31. Wigner, E. P. and Seitz, F. Qualitative analysis of the cohesion in metals. In Seitz, F. and Turnbull, D., eds. Solid state physics. Vol. 1, pp. 97-126. New York, N. Y., Academic Press, Inc. 1955.

32. Trulson, O. C. Cohesive energies of some rare earth metals. Unpublished Ph.D. Thesis. Ames, Iowa, Library, Iowa State University of Science and

Technology. 1959.

33. Landholt-Bornstein, H. H. Zahlenwerte und funktionen. 6th ed. Vol. 1. Berlin, J. Springer. 1955.

34. Pauling, L. and Sherman, J. Z. Krist. 81, 1 (1932).

35. Ewald, P. P. Ann. Physik 64, 253 (1921).

36. Meyerhoff, R. W. Anisotropic thermal expansion of zinc, beryllium, and yttrium single crystals at low temperatures. Unpublished M.S. Thesis. Ames, Iowa, Library, Iowa State University of Science and Technology. 1959.

37. Huntington, H. B. The elastic constants of crystals. In Seitz, F. and Turnbull, D., eds. Solid state physics. Vol. 7, pp. 213-351. New York, N. Y., Academic Press, Inc. 1958.

38. Hall, P. W. Electrical resistivity of yttrium and dysprosium single crystals. Unpublished Ph.D. Thesis. Ames, Iowa, Library, Iowa State University of Science and Technology. 1959.

VII. ACKNOWLEDGMENTS

The author wishes to thank Dr. J. F. Smith for suggesting the problem and for his guidance and encouragement throughout the course of this work. Thanks are due to Dr. J. M. Keller for his critical appraisal of this work and his helpful suggestions. The author wishes to extend his thanks to Dr. J. R. Reitz for supplying some of the necessary information and to Miss Nadine Tersene for her help with some of the calculations. Special thanks are due the authors wife Claire for her kindness and understanding during the course of this problem.

VIII. APPENDIX

A. First and Second Derivatives of the Direct and Reciprocal Lattice Vectors with Respect to the Strain Parameters ξ, η, and ϵ

The direct and reciprocal lattice vectors are defined respectively as

$$\hat{R}_1 = n_1\hat{a}_1 + n_2\hat{a}_2 + n_3\hat{a}_3$$

and

$$\hat{h}_1 = k_1\hat{b}_1 + k_2\hat{b}_2 + k_3\hat{b}_3 .$$

The following quantities are defined for a hexagonal close-packed crystal:

$$s = n_1^2 - n_1n_2 + n_2^2 ,$$

$$m = (c/a)^2 n_3^2 ,$$

$$s' = k_1^2 + k_1k_2 + k_3^2 ,$$

$$m' = (a/c)^2 k_3^2 .$$

For the shear corresponding to C the derivatives of the direct and reciprocal lattice vectors with respect to the strain parameter ξ are given by the relations:

$$\left(\frac{dR_1}{d\xi}\right)_{\xi=1} = \frac{1}{3}\, a\, \frac{(s - 2m)}{(s + m)^{\frac{1}{2}}} ,$$

$$\left(\frac{d^2R_1}{d\xi^2}\right)_{\xi=1} = -\frac{1}{9}\, a\, \frac{(2s^2 - 17ms - 10m^2)}{(s + m)^{3/2}} ,$$

$$\left(\frac{dh_1^2}{d\xi}\right)_{\xi=1} = \frac{1}{9a^2}\,(12m' - 8s') ,$$

$$\left(\frac{d^2h_1^2}{d\xi^2}\right)_{\xi=1} = \frac{1}{27a^2}\,(40s' + 12m') .$$

For the shear corresponding to C' the derivatives of the direct and reciprocal lattice vectors with respect to the strain parameter η are given by the relations:

$$\left(\frac{dR_1}{d\eta}\right)_{\eta=1} = \frac{a}{2}\, \frac{(n_1^2 - n_1n_2 - \frac{1}{2}n_2^2)}{(s + m)^{\frac{1}{2}}} ,$$

$$\left(\frac{d^2R_1}{d\eta^2}\right)_{\eta=1} = a\, \left[\frac{3}{4}\, \frac{n_2^2}{(s + m)^{\frac{1}{2}}} - \frac{(n_1^2 - n_1n_2 - \frac{1}{2}n_2^2)^2}{4(s + m)^{3/2}}\right] ,$$

$$\left(\frac{dh_1^2}{d\eta}\right)_{\eta=1} = \frac{1}{a^2}\, \left[\frac{4}{3}(k_2^2 + k_1k_2) - \frac{2}{3}k_1^2\right] ,$$

$$\left(\frac{d^2h_1^2}{d\eta^2}\right)_{\eta=1} = \frac{2}{a^2}k_1^2 .$$

For the shear corresponding to C" the derivatives of the direct and reciprocal lattice vectors with respect to the strain parameter ϵ are given by the relations:

$$\left(\frac{dR_1}{d\epsilon}\right)_{\epsilon=0} = \frac{a}{2}(c/a)\,\frac{(2n_1n_3 - n_2n_3)}{(s+m)^{\frac{1}{2}}} ,$$

$$\left(\frac{d^2R_1}{d\epsilon^2}\right)_{\epsilon=0} = a\,\frac{(n_1^2 - n_1n_2 + \frac{1}{4}n_2^2)}{(s+m)^{\frac{1}{2}}} - \frac{(c/a)^2(2n_1n_3-n_2n_3)^2}{4(s+m)^{3/2}} ,$$

$$\left(\frac{dh_1^2}{d\epsilon}\right)_{\epsilon=0} - \frac{2k_1k_3}{a^2}\,(a/c) ,$$

$$\left(\frac{d^2h_1^2}{d\epsilon^2}\right)_{\epsilon=0} = \frac{2k_3^2}{a^2}\,(a/c)^2 .$$

B. Full Zone Contributions to the Elastic Shear Constant C

The full zone contributions to the elastic shear constant C were obtained by use of the data from Table 7 and differentiation of equation 80.

The contribution to C by 24 tetrahedra of type 1 is

$$\frac{9}{2}\left(\frac{d^2W_F^I}{d\xi^2}\right)_{\xi=1} = \frac{9\alpha_o h^2}{10\sqrt{3}ma^5}\,(a/c)\Big[\,0.8230 + 0.7901\,(a/c)^2 - 27.6667\,(a/c)^4 + 23.1111\,(a/c)^6 + 10.8854\,(a/c)^8\,\Big] .$$

The contribution to C by 48 tetrahedra of type 2 is

$$\frac{9}{2}\left(\frac{d^2W_F^I}{d\xi^2}\right)_{\xi=1} = \frac{9\alpha_o h^2}{10\sqrt{3}ma^5}\,(a/c)\Big[\,1.5638 + 0.6420\,(a/c)^2$$

$$- 2.9167\ (a/c)^4 - 18.0556\ (a/c)^6$$

$$- 6.5313\ (a/c)^8 \Big] .$$

The contribution to C by 48 tetrahedra of type 3 is

$$\frac{9}{2}\left(\frac{d^2 W_F^I}{d\xi^2}\right)_{\xi=1} = \frac{9\alpha_o h^2}{30\sqrt{3}ma^5}\,(a/c)\,\frac{1}{x^2}\Big[\ 1.7284 + 1.6379\ (a/c)^2$$

$$+ 22.4691\ (a/c)^4 + 17.3333\ (a/c)^6$$

$$+ \frac{1}{x}\Big(2.0741\ (a/c)^2 - 54.0494\ (a/c)^4$$

$$- 88.5926\ (a/c)^6 - 32\ (a/c)^8 \Big)$$

$$+ \frac{1}{x^2}\Big(37.3333\ (a/c)^4 + 88.4444\ (a/c)^6$$

$$+ 6.9333\ (a/c)^8 + 18\ (a/c)^{10} \Big) \Big] ,$$

where $x = \left(1 + (a/c)^2\right)$.

The contribution to C by 48 tetrahedra of type 4 is

$$\frac{9}{2}\left(\frac{d^2 W_F^I}{d\xi^2}\right)_{\xi=1} = \frac{18\alpha_o h^2}{30\sqrt{3}ma^5}\,(a/c)\,\frac{1}{x^2}\Big[\ 1.7284 + 2.6996\ (a/c)^2$$

$$+ 68.1636\ (a/c)^4 + 134.3333\ (a/c)^6$$

$$+ 81.2778\ (a/c)^8 + 14.5833\ (a/c)^{10}$$

$$+ \frac{1}{x}\Big(2.0741\ (a/c)^2 - 89.0864\ (a/c)^4$$

$$- 116.8519\ (a/c)^6 - 271.2500\ (a/c)^8$$

$$- 109.6667\ (a/c)^{10} - 14.7300\ (a/c)^{12}\Big)$$

$$+ \frac{1}{x^2}\Big(37.3333\ (a/c)^4 + 145.7778\ (a/c)^6$$

$$+ 210.3333\ (a/c)^8 + 139.5000\ (a/c)^{10}$$

$$+ 42\ (a/c)^{12} + 4.5\ (a/c)^{14}\Big)\Big],$$

where $x = \left(1 + (a/c)^2\right)$.

The contribution to C by 24 tetrahedra of type 5 is

$$\frac{9}{2}\left(\frac{d^2 W_F^I}{d\xi^2}\right)_{\xi=1} = -\frac{9\alpha_o h^2}{20\sqrt{3}ma^5}(a/c)\left[1.7284 + 0.0741\ (a/c)^2\right].$$

The contribution to C by 24 tetrahedra of type 6 is

$$\frac{9}{2}\left(\frac{d^2 W_F^I}{d\xi^2}\right)_{\xi=1} = \frac{9\alpha_o h^2}{60\sqrt{3}ma^5}(a/c)\,\frac{1}{x^2}\Big[\, y^{\frac{1}{2}}\Big(1.7284$$

$$+ 0.8971\ (a/c)^2 + 3.3889\ (a/c)^4\Big)$$

$$+ y^{-\frac{1}{2}}\Big(-1.556\ (a/c)^2 + 33.8704\ (a/c)^4$$

$$+ 69.0278\ (a/c)^6 + 21.7500\ (a/c)^8\Big)$$

$$- y^{-3/2}\Big(14\ (a/c)^4 + 60.1667\ (a/c)^6$$

$$+ 90.5000\ (a/c)^8 + 54.3750\ (a/c)^{10}$$

$$+ 10.1250\ (a/c)^{12}\Big) + \frac{y^{\frac{1}{2}}}{x}\Big(1.7778\ (a/c)^2$$

$$- 29.6049\ (a/c)^4 - 15.3333\ (a/c)^6\Big)$$

$$- \frac{y^{-\frac{1}{2}}}{x} \left(42.6667\ (a/c)^4 + 92.2963\ (a/c)^6 \right.$$
$$\left. + 49.8611\ (a/c)^8 + 18.0000\ (a/c)^{10} \right)$$
$$+ \frac{y^{\frac{1}{2}}}{x^2} \left(42.6667\ (a/c)^4 + 48.4444\ (a/c)^6 \right.$$
$$\left. + 12.0000\ (a/c)^8 \right) \Bigg],$$

where

$$x = \left(1 + (a/c)^2 \right),$$
$$y = \left(1 + 3(a/c)^2 + 9/4(a/c)^4 \right).$$

The contribution to C by 24 tetrahedra of type 7 is

$$\frac{9}{2} \left(\frac{d^2 W_F^I}{d\xi^2} \right)_{\xi=1} = \frac{9 \alpha_o h^2}{30\sqrt{3} m a^5} (a/c) \frac{1}{x^2} \Bigg[y^{\frac{1}{2}} \left(1.7284 \right.$$
$$\left. + 1.9588\ (a/c)^2 + 29.8148\ (a/c)^4 \right.$$
$$\left. + 28.8889\ (a/c)^6 + 11.6111\ (a/c)^8 \right)$$
$$+ y^{-\frac{1}{2}} \left(-1.5556\ (a/c)^2 + 12.9629\ (a/c)^4 \right.$$
$$+ 200.5556\ (a/c)^6 + 193.8333\ (a/c)^8$$
$$\left. + 101.1250\ (a/c)^{10} + 19.8750\ (a/c)^{12} \right)$$
$$- y^{-3/2} \left(14\ (a/c)^4 + 81.6667\ (a/c)^6 \right.$$
$$+ 185\ (a/c)^8 + 204\ (a/c)^{10} + 113.6250\ (a/c)^{12}$$
$$\left. + 28.8750\ (a/c)^{14} + 5.0625\ (a/c)^{16} \right)$$

$$+ \frac{y^{\frac{1}{2}}}{x}\left(1.7778\ (a/c)^2 - 64.6420\ (a/c)^4 \right.$$
$$- 117.5556\ (a/c)^6 - 58.3333\ (a/c)^8$$
$$\left. -15.6667\ (a/c)^{10} + 6\ (a/c)^{12} \right)$$
$$- \frac{y^{-\frac{1}{2}}}{x}\left(42.6667\ (a/c)^4 + 165.7778\ (a/c)^6 \right.$$
$$+ 250.6667\ (a/c)^8 + 168\ (a/c)^{10} + 51\ (a/c)^{12}$$
$$\left. + 9\ (a/c)^{14} \right) + \frac{y^{\frac{1}{2}}}{x^2}\left(42.6667\ (a/c)^4 \right.$$
$$\left. + 105.7778\ (a/c)^6 + 92\ (a/c)^8 + 30\ (a/c)^{10} \right) \Bigg] ,$$

where

$$x = \left(1 + (a/c)^2 \right) ,$$

$$y = \left(1 + 3(a/c)^2 + 9/4(a/c)^4 \right) .$$

C. Full Zone Contributions to the Elastic Shear Constant C'

The contributions to the elastic shear constant C' from a completely filled Brillouin zone were evaluated from the relations in Table 8 and differentiation of equation 80 with respect to the strain parameter η .

The contribution to C' from 8 tetrahedra of type 1 is:

$$\left(\frac{d^2 W_F^I}{d\eta^2}\right)_{\eta=1} = \frac{\alpha_o h^2}{10\sqrt{3}ma^5}\Bigg[- 5.5000\,(a/c)^4 - 1.5000\,(a/c)^6 + x\Big(0.3333\,y^3 + \{0.3333 + 0.5000\,(a/c)^2\}\,y^2 + 0.4444 + 0.6667\,(a/c)^2 + 2.5000\,(a/c)^4\Big) + x^2\Big(- 2\,(a/c)^2 - 1.5000\,(a/c)^4\Big) + x^3 \Big(- 1.3333 - 0.6667\,(a/c)^2\Big) - 0.5000\,(a/c)^2\,y^3 + y^2\Big(-0.5000\,(a/c)^2 - 0.3750\,(a/c)^4\Big)\Bigg] ,$$

where

$$x = \left(1 - 3/4(a/c)^2\right),$$
$$y = \left(2/3 - \tfrac{1}{2}(a/c)^2\right).$$

The contribution to C' from 8 tetrahedra of type 2 is:

$$\left(\frac{d^2 W_F^I}{d\eta^2}\right)_{\eta=1} = \frac{\alpha_o h^2}{20\sqrt{3}ma^5}\,(a/c)\Big[1.4444 - 3.0000\,(a/c)^2 - 6.3645\,(a/c)^4 - 0.8322\,(a/c)^6 - 0.2442\,\left(\tfrac{a}{c}\right)^8\Big].$$

The contribution to C' from 8 tetrahedra of type 3 is:

$$\left(\frac{d^2 W_F^I}{d\eta^2}\right)_{\eta=1} = \frac{\alpha_o h^2}{20\sqrt{3}ma^5}\,(a/c)\Big[1.1111 + 2.0000\,(a/c)^4 - 1.6944\,(a/c)^6 + 0.6354\,(a/c)^8\Big].$$

The contribution to C' from 16 tetrahedra of type 4 is:

$$\left(\frac{d^2 W_F^I}{d\eta^2}\right)_{\eta=1} = \frac{\alpha_o h^2}{10\sqrt{3}ma^5}\left[- 2.1234 - 2.2222\ (a/c)^2 + 2.2500\ (a/c)^4 + 1.5833\ (a/c)^6 - 0.2813\ (a/c)^8 \right] .$$

The contribution to C' from 16 tetrahedra of type 5 is:

$$\left(\frac{d^2 W_F^I}{d\eta^2}\right)_{\eta=1} = \frac{\alpha_o h^2}{20\sqrt{3}ma^5}\ (a/c)\Big[\ x^2 y\left(2.6667 + 0.3333\ (a/c)^2\right) + xy\left(-2(a/c)^2 + 2.7708\ (a/c)^4 + 0.7500\ (a/c)^6\right) + x^2\left(-4.4167\ (a/c)^2 - 0.7500\ (a/c)^4 + 3.7500\ (a/c)^6\right) + y\left(0.1250\ (a/c)^4 + 0.1875\ (a/c)^6\right) + x\left(8(a/c)^2 + 0.3750\ (a/c)^6\right) + 0.2161\ xy^3 - 0.0092\ (a/c)^2 y^3 + 2.6249\ (a/c)^2 xy^2 + 0.6667\ (a/c)^4 y^2\Big] ,$$

where

$$x = \left(1 + 3/4(a/c)^2\right),$$
$$y = \left(1 - 3/4(a/c)^2\right).$$

The contribution to C' from 16 tetrahedra of type 6 is:

$$\left(\frac{d^2 W_F^I}{d\eta^2}\right)_{\eta=1} = \frac{\alpha_o h^2}{20\sqrt{3}ma^5}\ (a/c)\ \Big[x^2 y\left(2.6667 + 0.3333\ (a/c)^2\right)$$

$$- xy\left(2.6667\ (a/c)^2 + 0.5000\ (a/c)^4\right)$$

$$+ x^2\left(1.3333\ (a/c)^2 + 0.2500\ (a/c)^4\right)$$

$$+ y\left(0.5000\ (a/c)^4 + 0.9375\ (a/c)^6\right)$$

$$- x\left(0.9167\ (a/c)^4 + 0.5625\ (a/c)^6\right) + 0.3457\ xy^3$$

$$+ 0.0741\ (a/c)^2y^3 - 0.1667\ (a/c)^2xy^2$$

$$- 0.0833\ (a/c)^4y^2\Big] ,$$

where

$$x = \left(1 + 3/4(a/c)^2\right),$$
$$y = \left(1 - 3/4(a/c)^2\right).$$

The contribution to C' from 16 tetrahedra of type 7 is:

$$\left(\frac{d^2W_F^I}{d\eta^2}\right)_{\eta=1} = \frac{\alpha_o h^2}{20\sqrt{3}ma^5}\,(a/c)\left[\frac{1}{x}\left[\left(2.3704\ y^2 - 1.7778\ (a/c)^2y + 0.6667\ (a/c)^2\right)\right] + \frac{1}{x^2}\left(-0.3704\ (a/c)^2y^2 - 0.8889\ (a/c)^4y + 1.7778\ y^2 + 1.7778\ (a/c)^2y + 0.1728\ (a/c)^4\right) + \frac{1}{x^3}\left(\left\{-1.2840\ (a/c)^2 + 0.2963\ (a/c)^4\right\}y^2 - \left\{0.2880\ (a/c)^4 + 0.1481\right\}y + 0.0370\ (a/c)^6\right) + \frac{1}{x^4}\left(\left\{0.5926 - 0.4444\ (a/c)^4\right\}y^2 + 0.0370\ (a/c)^6y\right)\right] ,$$

where

$$x = \left(1 + (a/c)^2 \right),$$
$$y = \left(1 + 3/4(a/c)^2 \right).$$

The contribution to C' from 16 tetrahedra of type 8 is:

$$\left(\frac{d^2 W_F^I}{d\eta^2}\right)_{\eta=1} = \frac{\alpha_o h^2}{40\sqrt{3}ma^5} (a/c) \left[\frac{1}{x} \left(0.5926\, y^2 - 5.3333\, (a/c)^2 y + 0.3333\, (a/c)^4 \right) + \frac{1}{x^2} \left(\left\{ -0.4938 - 2.9630\, (a/c)^2 \right\} y^2 + \left\{ 0.1975\, (a/c)^2 + 0.9630\, (a/c)^4 \right\} y - 0.1019\, (a/c)^4 \right) + \frac{1}{x^3} \left(\left\{ -0.1975\, (a/c)^2 + 0.5926\, (a/c)^4 \right\} y^2 + 0.1481\, (a/c)^4 y + 0.0185\, (a/c)^6 \right) + \frac{1}{x^4} \left(0.2963\, (a/c)^4 y^2 + 0.0370\, (a/c)^6 y \right) \right],$$

where

$$x = \left(1 + (a/c)^2 \right),$$
$$y = \left(1 + 3/4(a/c)^2 \right).$$

The contribution to C' from 16 tetrahedra of type 9 is:

$$\left(\frac{d^2 W_F^I}{d\eta^2}\right)_{\eta=1} = \frac{\alpha_o h^2}{60\sqrt{3}ma^5} (a/c) \left[\frac{1}{x} \left(5.333\, y^2 + 2.6667\, (a/c)^2 y \right. \right.$$

$$+ 0.5000\ (a/c)^4\Big) + \frac{1}{x^2}\Big(4y^2 + \Big\{ 2.1728\ (a/c)^2 - 2.6667\ (a/c)^4 \Big\} y + 0.1852\ (a/c)^4 \Big) - \frac{1}{x^3}\Big(+ 1.1852\ (a/c)^2 y^2 + 1.5309\ (a/c)^4 y \Big) + \frac{1}{x^4}\Big(1.7778\ (a/c)^4 y^2 + 0.1481\ (a/c)^6 \Big)\Big],$$

where

$$x = \left(1 + (a/c)^2 \right),$$
$$y = \left(1 + 3/4(a/c)^2 \right).$$

The contribution to C' from 16 tetrahedra of type 10 is:

$$\left(\frac{d^2 W_F^I}{d\eta^2}\right)_{\eta=1} = \frac{\alpha_o h^2}{20\sqrt{3}ma^5}\ (a/c)\Bigg[\frac{1}{x}\Big(- 2.9630 + 1.7778\ (a/c)^2 yt + 1.7778\ (a/c)^2 y^2 + 1.3333\ (a/c)^4 t + 5.3333\ (a/c)^4 y + 0.2963\ (a/c)^2 y^2 t - 0.0658\ (a/c)^4 t^2 \Big) + \frac{1}{x^2}\Big(y^2 t \Big\{1.1852 - 2.5185\ (a/c)^2\Big\} + yt \Big\{3.5556\ (a/c)^2 - 1.1358\ (a/c)^4\Big\} + y^2\Big\{ - 0.0878 + 2.1111\ (a/c)^2 - 1.3333\ (a/c)^4\Big\} + y\Big\{0.8889\ (a/c)^4 + 0.2963\ (a/c)^6\Big\} + 0.1536\ (a/c)^2 yt^2 + t\Big\{0.0988\ (a/c)^4$$

$$+ 0.2963\ (a/c)^6\Big\}\Big) + \frac{1}{x^3}\Big(y^2t\Big\{1.1852\ (a/c)^2 + 0.2963\ (a/c)^4\Big\} + yt\Big\{-0.8889\ (a/c)^4 - 0.3951\ (a/c)^6\Big\} + 0.8889\ (a/c)^4y^2 + yt^2\Big\{-0.2634 + 0.1317\ (a/c)^4 - 0.0988\ (a/c)^6t\Big\}\Big) + \frac{1}{x^4}\Big(-0.5185\ (a/c)^4y^2t + 0.0988\ (a/c)^6yt^2\Big)\Big],$$

where

$$x = \Big(1 + (a/c)^2\Big),$$
$$y = \Big(1 + 3/4(a/c)^2\Big),$$
$$t = \Big(1 + 3/2(a/c)^2\Big).$$

The contribution to C' from 16 tetrahedra of type 11 is:

$$\Big(\frac{d^2W_F^I}{d\eta^2}\Big)_{\eta=1} = \frac{\alpha_o h^2}{40\sqrt{3}ma^5}(a/c)\Big[\frac{1}{x}\Big(2.6667\ y^2z - 2(a/c)^2yz + \Big\{1.1852 + 8.8889\ (a/c)^2\Big\}y^2 + \Big\{-1.3333\ (a/c)^2 - 0.6667\ (a/c)^4\Big\}y + 0.7500\ (a/c)^4z\Big) + \frac{1}{x^2}\Big(y^2z\Big\{1.0370 - 3.5556\ (a/c)^2 + 0.8889\ (a/c)^4\Big\} + yz\Big\{0.9259\ (a/c)^2 - (a/c)^6\Big\} + y^2(1.1852) + 0.1250\ (a/c)^4z + 0.6667\ (a/c)^4y + 0.2707\ (a/c)^6z^3$$

$$+ yz^2\left\{0.2222\ (a/c)^2 + 0.6667\ (a/c)^4 + 0.3333\ (a/c)^6\right\} + z^2\left\{0.0833\ (a/c)^4 + 0.1250\ (a/c)^6\right\}\Bigg) + \frac{1}{x^3}\Bigg(y^2z - 1.1852\ (a/c)^2 + 0.5556\ (a/c)^4yz + y^2\left\{0.3951\ (a/c)^2 - 0.5926\ (a/c)^4\right\} - 0.1111\ (a/c)^4z^3y + 0.0417\ (a/c)^6z^3 + yz^2\left\{0.1111\ (a/c)^4 - 0.6667\ (a/c)^6\right\}\Bigg) + \frac{1}{x^4}\Bigg(- 0.4444\ (a/c)^4y^2z + yz^3\left\{-0.3333\ (a/c)^2 + 0.4167\ (a/c)^6\right\}\Bigg)\Bigg],$$

where

$$x = \left(1 + (a/c)^2\right),$$
$$y = \left(1 + 3/4(a/c)^2\right),$$
$$z = \left(4/3 + 2(a/c)^2\right).$$

The contribution to C' from 16 tetrahedra of type 12 is:

$$\left(\frac{d^2W_F^I}{d\eta^2}\right)_{\eta=1} = \frac{\alpha\, o h^2}{20\sqrt{3}ma^5}\,(a/c)\left[\frac{1}{y}\left(3.3333\ (a/c)^4 + x^2t\left\{1.1852 + 0.8889\ (a/c)^2\right\} - 4.4444\ (a/c)^2xt - 3.1111\ (a/c)^2x^2 + 0.3333\ (a/c)^4t + x\left\{3.5556\ (a/c)^2 + 2.6667\ (a/c)^4\right\}\right)\right.$$

$$+\frac{1}{y^2}\Big(-4.1481\,(a/c)^4x^2+xt\{0.1481\,(a/c)^2-1.7778\,(a/c)^4\}-3.4074\,(a/c)^4x+0.0556\,(a/c)^4t-0.1481\,(a/c)^2xt^3-0.4352\,(a/c)^4t^3-0.4444\,(a/c)^4xt^2+0.6667\,(a/c)^6t^2+4(a/c)^6xt\Big)$$

$$+\frac{1}{y^3}\Big(x^2t\{-0.7901\,(a/c)^2+2.3704\,(a/c)^4\}-0.5926\,(a/c)^4xt-1.7778\,(a/c)^4x^2+0.5926\,(a/c)^4xt^3-0.1481\,(a/c)^6t^3-3.5556\,(a/c)^6xt^2\Big)+\frac{1}{y^4}\Big(1.1852\,(a/c)^4x^2t+0.5926\,(a/c)^6xt^3\Big)\Big],$$

where

$$x=\left(1+3/4(a/c)^2\right),$$
$$y=\left(1+(a/c)^2\right),$$
$$t=\left(1+3/2(a/c)^2\right).$$

The contribution to C' from 12 tetrahedra of type 13 is:

$$\left(\frac{d^2W_F^I}{d\eta^2}\right)_{\eta=1}=-\frac{3\alpha_o h^2}{40\sqrt{3}ma^5}(a/c)\left[0.4444-0.1111\,(a/c)^2\right].$$

The contribution to C' from 12 tetrahedra of type 14 is:

$$\left(\frac{d^2 W_F^I}{d\eta^2}\right)_{\eta=1} = \frac{3\alpha_o h^2}{40\sqrt{3}ma^5}(a/c)\left[\frac{1}{x}\left(y^{\frac{1}{2}}\left\{-2.6667 + 2.6667\,(a/c)^2\right\} + y^{-\frac{1}{2}}\left\{0.7901 - 1.1852\,(a/c)^2 - 1.7778\,(a/c)^4 + 2.6667\,(a/c)^6\right\} + y^{-1}\left\{-0.2364 + 1.1852\,(a/c)^4 - 1.3333\,(a/c)^8\right\} - 1.1852 - 2.6667\,(a/c)^2 + 4.0000\,(a/c)^4\right) + \frac{1}{x^2}\left(y^{\frac{1}{2}}\left\{0.8889 + 0.5925\,(a/c)^2 - 5.0000\,(a/c)^4 + 2.3333\,(a/c)^6 + (a/c)^8\right\} + y\left\{1.3333 - 5.2222\,(a/c)^2 - 3.1666\,(a/c)^4 + 1.6667\,(a/c)^6\right\} - 0.3333\,(a/c)^2 y^{3/2} + y^2 + 0.2963 + 0.1152\,(a/c)^2 - 1.3333\,(a/c)^4 - 5.6667\,(a/c)^6 + 1.5000\,(a/c)^8 + 0.1667\,(a/c)^{10}\right) + \frac{1}{x^3}\left(y^2\left\{0.5000\,(a/c)^2 + 0.2222\,(a/c)^4 - 0.5000\,(a/c)^8\right\} + y^{3/2}\left\{(a/c)^2 - 0.5000\,(a/c)^4 - 1.5000\,(a/c)^6\right\} + y\left\{2.0000\,(a/c)^2 + 2.6667\,(a/c)^4\right.\right.$$

$$- 4.5000\ (a/c)^6 \Big\} \Big) + \frac{1}{x^4} \Big(y^2 \Big\{ 1.5000\ (a/c)^4 + 0.5000\ (a/c)^6 \Big\} \Big) \Big],$$

where

$$x = \Big(1 + (a/c)^2 \Big),$$
$$y = \Big(4/9 + 4/3(a/c)^2 + (a/c)^4 \Big).$$

The contribution to C' from 12 tetrahedra of type 15 is:

$$\left(\frac{d^2 W_F^I}{d\eta^2}\right)_{\eta=1} = \frac{\alpha_o h^2}{40\sqrt{3}ma^5}\,(a/c) \Bigg[\frac{1}{x} \Big(8y^{\frac{1}{2}} + y^{-\frac{1}{2}} \Big\{ - 3.5556 - 2.6667\ (a/c)^2 + 9.3333\ (a/c)^4 \Big\} + y^{-3/2} \Big\{ - 0.2634 + 1.1852\ (a/c)^4 - 1.3333\ (a/c)^8 \Big\} \Big) + \frac{1}{x^2} \Big(y^{\frac{1}{2}} \Big\{ - 1.3333 - 10.4444\ (a/c)^2 + 4.5000\ (a/c)^4 \Big\} + y^{-\frac{1}{2}} \Big\{ 0.2963 + 1.0864\ (a/c)^2 - 1.0741\ (a/c)^4 - 2.4259\ (a/c)^6 + 1.500\ (a/c)^8 \Big\} + y^{-3/2} \Big\{ - 0.0037\ (a/c)^2 + 0.0082\ (a/c)^4 + 0.0082\ (a/c)^6 - 0.0185\ (a/c)^{10} \Big\} \Big) + \frac{1}{x^3} \Big(y^{\frac{1}{2}} \Big\{ 2.6667\ (a/c)^2 + 2.2222\ (a/c)^4$$

$$- 6(a/c)^6 \Big\} - 2(a/c)^2 y^{3/2} + y^{-\frac{1}{2}} \Big\{0.0329\ (a/c)^4 - 0.0740\ (a/c)^8 \Big\}\Big) + \frac{1}{x^4}\left(3(a/c)^4 y^{3/2} + \frac{1}{9}(a/c)^6 y^{\frac{1}{2}}\right)\Big],$$

where

$$x = \left(1 + (a/c)^2\right),$$
$$y = \left(4/9 + 4/3(a/c)^4\right).$$

The contribution to C' from 12 tetrahedra of type 16 is:

$$\left(\frac{d^2 W_F^I}{d\eta^2}\right)_{\eta=1} = -\frac{3\alpha_o h^2}{80\sqrt{3}ma^5}(a/c)\left[7.2593 - 0.1111\ (a/c)^2\right].$$

The contribution to C' from 12 tetrahedra of type 17 is:

$$\left(\frac{d^2 W_F^I}{d\eta^2}\right)_{\eta=1} = \frac{\alpha_o h^2}{80ma^5}(a/c)\Bigg[\frac{1}{x}\Big(2.6667\ y^{\frac{1}{2}} + y^{-\frac{1}{2}}\Big\{0.0741 + 1.5556\ (a/c)^4\Big\} + y^{-3/2}\Big\{-0.0329 + 0.1667\ (a/c)^8\Big\}\Big) + \frac{1}{x^2}\Big(y^{\frac{1}{2}}\Big\{-0.2963 - 3.5370\ (a/c)^2 + 3.1111\ (a/c)^4\Big\} + y^{-\frac{1}{2}}\Big\{0.0494 - 0.1811\ (a/c)^2 - 0.2222\ (a/c)^4 + 0.0324\ (a/c)^6 + 0.25\ (a/c)^8\Big\} - 0.4444\ y^{3/2}\Big) + \frac{1}{x^3}\Big(y^{\frac{1}{2}}\Big\{-0.2963 + 0.9383\ (a/c)^2$$

$$+ 1.0370\ (a/c)^4 - 2(a/c)^6 \Big\} + y^{3/2} \Big\{ 0.2963 - 2.6667\ (a/c)^2 \Big\} \Big) \frac{1}{x^4} \Big(y^{3/2} \Big\{ - 0.2963\ (a/c)^2 + 1.7778\ (a/c)^4 \Big\} \Big) \Big],$$

where

$$x = \left(1 + (a/c)^2 \right),$$
$$y = \left(0.3333 + (a/c)^2 + 0.75\ (a/c)^4 \right).$$

The contribution to C' from 12 tetrahedra of type 18 is:

$$\left(\frac{d^2 W_F^I}{d\eta^2}\right)_{\eta=1} = \frac{\alpha_o h^2}{80ma^5}\ (a/c) \Bigg[\frac{1}{x} \Big(5.3333\ y^{\frac{1}{2}}t + 1.7778\ (a/c)^4 y^{-\frac{1}{2}}t + 7.1111\ (a/c)^2 y^{\frac{1}{2}} + y^{-3/2}t \Big\{ 0.0658 - 0.2963\ (a/c)^4 + 0.6667\ (a/c)^8 \Big\} + y^{-\frac{1}{2}} \Big\{ - 0.5926\ (a/c)^2 + 2.6667\ (a/c)^6 \Big\} \Big) + \frac{1}{x^2} \Big(y^{\frac{1}{2}}t \Big\{ 1.1852 - 4.1481\ (a/c)^2 - 1.1852\ (a/c)^4 + 1.7778\ (a/c)^6 \Big\} + y^{-\frac{1}{2}}t \Big\{ 0.0988 + 0.3951\ (a/c)^2 - 0.8889\ (a/c)^4 - 1.3333\ (a/c)^6 + 0.5\ (a/c)^8 \Big\} + y^{\frac{1}{2}} \Big\{ - 1.7778 (a/c)^2 - 3.5555\ (a/c)^4 + 4(a/c)^6 \Big\} + 2.6667\ y^{3/2}t + 0.4938\ (a/c)^2 y^{\frac{1}{2}}t^3 + y^{-\frac{1}{2}}t^3 + y^{-\frac{1}{2}}t^3 \Big\{ 0.1394\ (a/c)^2$$

$$- 0.0494\ (a/c)^6\Big\} - 0.5926\ (a/c)^4 y^{\frac{1}{2}} t^2$$

$$+ y^{-\frac{1}{2}} t^2 \Big\{ - 0.1975\ (a/c)^4 + 0.4444\ (a/c)^8 \Big\}$$

$$+ y^{-3/2} t^3 \Big\{ - 0.0037\ (a/c) + 0.0165\ (a/c)^6$$

$$- 0.0185\ (a/c)^{10} \Big\} \Big) + \frac{1}{x^3} \Big(y^{\frac{1}{2}} t \Big\{ 1.1852\ (a/c)^2$$

$$+ 2.3704\ (a/c)^4 - 2.6667\ (a/c)^6 \Big\}$$

$$- 1.1852\ (a/c)^2 y^{3/2} t - 0.3786\ (a/c)^4 y^{\frac{1}{2}} t^3$$

$$- 1.1852\ (a/c)^6 y^{\frac{1}{2}} t^2 + y^{-\frac{1}{2}} t^3 \Big\{ 0.0439\ (a/c)^4$$

$$- 0.0988\ (a/c)^8 \Big\} \Big) + \frac{1}{x^4} \Big(1.7778\ (a/c)^4 y^{3/2} t$$

$$+ 0.1975\ (a/c)^6 y^{\frac{1}{2}} t^3 \Big) \Big],$$

where

$$x = \left(1 + (a/c)^2 \right),$$

$$y = \left(1/3 + (a/c)^2 + 3/4(a/c)^4 \right),$$

$$t = \left(1 + 3/2(a/c)^2 \right).$$

D. Relations for the Determination of the Change in Electrostatic, Non-Coulomb Repulsive, and Full Zone Energies with Strain

The change in the electrostatic energy with respect to the strain parameter ξ is given by the relation:

$$\left(\frac{dE_1}{d\xi}\right)_{\xi=1} = \frac{e^2}{2}\left[\frac{1}{\pi\Omega}\left\{\sum_1{}' \left(\frac{-\pi^2}{h_1^2} - \frac{1}{h_1^4}\right)\left(\frac{dh_1^2}{d\xi}\right)_{\xi=1} \exp\left(\frac{-\pi^2 h_1^2}{E^2}\right)\right\} + \left\{\sum_1{}' (-2E^2)\left(\frac{2}{\sqrt{\pi}}\right)\left(\frac{dR_1}{d\xi}\right)_{\xi=1} \exp\left(-E^2R_1^2\right) - \left(\frac{1 - \phi(ER_1)}{R_1^2}\right)\left(\frac{dR_1}{d\xi}\right)_{\xi=1}\right\}\right].$$

The change in the non-Coulomb core repulsive energy with respect to the strain parameter is given by the relation:

$$\left(\frac{dE_I}{d\xi}\right)_{\xi=1} = \frac{1}{2} \sum_{R_1} \left(\frac{dW_R}{dR_1}\right)_{\xi=1} \left(\frac{dR_1}{d\xi}\right)_{\xi=1} .$$

The change in the full zone energy with respect to the strain parameter ξ may be evaluated by differentiation of equation 80 using the relations for p, q, and r given in Table 7.

For 24 tetrahedra of type 1:

$$\left(\frac{dW_F^I}{d\xi}\right)_{\xi=1} = \frac{\alpha_o h^2}{5\sqrt{3}ma^5}(a/c)\left[-0.4938 + 2.3704\,(a/c)^2 - 11.6667\,(a/c)^4 + 5.3333\,(a/c)^6 + 1.7188\left(\frac{a}{c}\right)^8\right].$$

For 48 tetrahedra of type 2:

$$\left(\frac{dW_F^I}{d\xi}\right)_{\xi=1} = \frac{\alpha_o h^2}{5\sqrt{3}ma^5}(a/c)\left[-0.9383 + 1.9259\,(a/c)^2 - 1.2500\,(a/c)^4 - 4.1667\,(a/c)^6 - 1.0313\,(a/c)^8\right].$$

For 48 tetrahedra of type 3:

$$\left(\frac{dW_F^I}{d\xi}\right)_{\xi=1} = \frac{\alpha_o h^2}{15\sqrt{3}ma^5}(a/c)\,\frac{1}{x^2}\left[-1.0370 + 4.9136\,(a/c)^2 + 9.6296\,(a/c)^4 + 4.0000\,(a/c)^6 - \frac{1}{x}\left(6.2222\,(a/c)^2 + 14.7407\,(a/c)^4 + 11.5556\,(a/c)^6 + 3.0000\,(a/c)^8\right)\right],$$

where $x = \left(1 + (a/c)^2\right)$.

For 48 tetrahedra of type 4:

$$\left(\frac{dW_F^I}{d\xi}\right)_{\xi=1} = \frac{2\alpha_o h^2}{15\sqrt{3}ma^5}(a/c)\,\frac{1}{x^2}\left[-1.0370 + 8.0987\,(a/c)^2 + 29.2130\,(a/c)^4 + 31.0000\,(a/c)^6 + 12.8333\,(a/c)^8 + 1.7500\,(a/c)^{10} - \frac{1}{x}\left(6.2222\,(a/c)^2 + 24.2963\,(a/c)^4 + 35.0556\,(a/c)^6 + 23.2500\,(a/c)^8 + 7.0000\,(a/c)^{10} + 0.7500\,(a/c)^{12}\right)\right],$$

where $x = \left(1 + (a/c)^2 \right)$.

For 24 tetrahedra of type 5:

$$\left(\frac{dW_F^I}{d\xi}\right)_{\xi=1} = - \frac{\alpha_o h^2}{10\sqrt{3}ma^5} (a/c) \left[1.0370 - 2.2222 (a/c)^2 \right] .$$

For 24 tetrahedra of type 6:

$$\begin{aligned}\left(\frac{dW_F^I}{d\xi}\right)_{\xi=1} = \frac{\alpha_o h^2}{20\sqrt{3}ma^5} (a/c) \frac{1}{x^2} \Bigg[& y^{\frac{1}{2}} \Big(- 1.0370 \\ & + 2.6914 (a/c)^2 + 1.6667 (a/c)^4 \Big) \\ & + y^{-\frac{1}{2}} \Big(4.6667 (a/c)^2 + 13.0556 (a/c)^4 \\ & + 10.5833 (a/c)^6 + 2.2500 (a/c)^8 \Big) \\ & - \frac{y^{\frac{1}{2}}}{x} \Big(7.1111 (a/c)^2 + 8.0741 (a/c)^4 \\ & + 2.0000 (a/c)^6 \Big) \Bigg] ,\end{aligned}$$

where

$$x = \left(1 + (a/c)^2 \right) ,$$
$$y = \left(1 + 3(a/c)^2 + 9/4(a/c)^4 \right) .$$

For 24 tetrahedra of type 7:

$$\left(\frac{dW_F^I}{d\xi}\right)_{\xi=1} = \frac{\alpha_o h^2}{15\sqrt{3}ma^5} (a/c) \frac{1}{x^2} \Bigg[y^{\frac{1}{2}} \Big(- 1.0370$$

$$+ 5.8765\,(a/c)^2 + 12.7778\,(a/c)^4 + 6.6667\,(a/c)^6$$
$$+ 1.8333\,(a/c)^8 \Big) + y^{-\frac{1}{2}} \Big(4.6667\,(a/c)^2$$
$$+ 20.2222\,(a/c)^4 + 31.3333\,(a/c)^6 + 21.0000\,(a/c)^8$$
$$+ 6.3750\,(a/c)^{10} + 1.1250\,(a/c)^{12} \Big)$$
$$- \frac{y^{\frac{1}{2}}}{x} \Big(7.1111\,(a/c)^2 + 17.6296\,(a/c)^4$$
$$+ 15.3333\,(a/c)^6 + 5.0000\,(a/c)^8 + (a/c)^{10} \Big) \Big],$$

where

$$x = \left(1 + (a/c)^2\right),$$
$$y = \left(1 + 3(a/c)^2 + 9/4(a/c)^4\right).$$